Published in final edited form as:
J Chem Neuroanat. 2013 May ; 0: 21–38. doi:10.1016/j.jchemneu.2013.02.007.

Differential expression of vesicular glutamate transporters 1 and 2 may identify distinct modes of glutamatergic transmission in the macaque visual system

Pooja Balaram, B.Sc.,
Vanderbilt University, Dept. of Psychology

Troy A. Hackett, Ph.D., and
Vanderbilt University School of Medicine, Dept. of Hearing and Speech Sciences, Dept. of Psychology

Jon H. Kaas, Ph.D.
Vanderbilt University, Dept. of Psychology, Dept. of Cell and Molecular Biology

Abstract

Glutamate is the primary neurotransmitter utilized by the mammalian visual system for excitatory neurotransmission. The sequestration of glutamate into synaptic vesicles, and the subsequent transport of filled vesicles to the presynaptic terminal membrane, is regulated by a family of proteins known as vesicular glutamate transporters (VGLUTs). Two VGLUT proteins, VGLUT1 and VGLUT2, characterize distinct sets of glutamatergic projections between visual structures in rodents and prosimian primates, yet little is known about their distributions in the visual system of anthropoid primates. We have examined the mRNA and protein expression patterns of VGLUT1 and VGLUT2 in the visual system of macaque monkeys, an Old World anthropoid primate, in order to determine their relative distributions in the superior colliculus, lateral geniculate nucleus, pulvinar complex, V1 and V2. Distinct expression patterns for both VGLUT1 and VGLUT2 identified architectonic boundaries in all structures, as well as anatomical subdivisions of the superior colliculus, pulvinar complex, and V1. These results suggest that VGLUT1 and VGLUT2 clearly identify regions of glutamatergic input in visual structures, and may identify common architectonic features of visual areas and nuclei across the primate radiation. Additionally, we find that VGLUT1 and VGLUT2 characterize distinct subsets of glutamatergic projections in the macaque visual system; VGLUT2 predominates in driving or feedforward projections from lower order to higher order visual structures while VGLUT1 predominates in modulatory or feedback projections from higher order to lower order visual structures. The distribution of these two proteins suggests that VGLUT1 and VGLUT2 may identify class 1 and class 2 type glutamatergic projections within the primate visual system (Sherman and Guillery, 2006).

Keywords

VGLUT; primate; visual cortex; lateral geniculate nucleus; superior colliculus; pulvinar

Correspondence to: Pooja Balaram, Vanderbilt University, 301 Wilson Hall, 111 21st Avenue South, Nashville, TN 37203, Phone: 508-314-3030, Fax: 615-343-8449, pooja.balaram@vanderbilt.edu.

1. Introduction

The primate visual system consists of an intricate network of brain structures that process visual information (Casagrande and Kaas, 1994; Felleman and Van Essen, 1991; Krubitzer and Kaas, 1989; Salin and Bullier, 1995; Valverde, 1985; Van Essen, 1985, 2005). The dense connections that interlink individual visual structures have been examined through tracer studies that define projections to and from given areas and nuclei. However, the neuronal populations that give rise to individual projections in the visual system are often morphologically indistinct from each other, making it difficult to characterize the types of neurons that comprise a single projection (Levitt et al, 1996; Lund et al, 1978, 1988). The use of cellular and genetic markers to identify discrete populations of cells now allows us to isolate neurons that express a unique marker and correlate their connections and functional attributes within sensory systems (Baldwin et al, 2011; Bernard et al, 2012; Hevner et al, 2007; Lein et al, 2007;). Thus, groups of neurons that give rise to distinct visual projections can now be classified based on their genetic and molecular characteristics. Since these molecular markers are also intrinsically tied to cellular processes, their expression patterns may identify neuronal properties that give rise to specific functions within a neuronal circuit as well (Fremeau et al, 2004; Hevner, 2003; Kubota and Kawaguchi, 1994; Yamamori, 2011). Thus, the diversity of genetic and molecular markers within neurons of the primate visual system could contribute to the range of neuronal responses within visual circuits. The molecular characterization of excitatory neurons and neuronal circuits in the primate visual system depends, in large part, on the use of glutamate as an excitatory neurotransmitter. However, the identification of glutamate within a neuron is not enough to classify it as glutamatergic, since glutamate is a ubiquitous amino acid in most cells of the nervous system. The classification of glutamate as a signaling molecule within a neuron requires the identification of a glutamate transporter, a protein responsible for containing glutamate within secretory vesicles that are released upon signal transmission (Danbolt et al, 1994; Davanger et al, 2009; Reimer et al, 2001). A family of such transport proteins, the vesicular glutamate transporters (VGLUTs), have been identified in the mammalian central nervous system (Aihara et al, 2000; Bellocchio et al, 2000; Bryant et al, 2012; Gras et al, 2002; Hackett et al, 2011; Hackett and de la Mothe, 2009; Herzog et al, 2001; Fyk-Kolodziej et al, 2004; Kaneko and Fujiyama 2001) and are known to contribute to glutamatergic signaling within neuronal circuits (Fremeau, 2004; Fremeau et al 2001; Santos, 2009; Varoqui et al, 2002). Thus, VGLUT expression characterizes a glutamatergic phenotype in neuronal populations.

Two VGLUT isoforms, VGLUT1 and VGLUT2, are widely distributed across the mammalian brain, and appear to distinguish separate types of projections between and within parts of the visual system (Balaram et al, 2011a, 2011b; Baldwin et al, 2011; Fremeau et al, 2004; Fyk-Kolodziej et al, 2004; Garcia-Marin et al, 2013; Hackett et al, 2011; Herzog et al, 2001; Kaneko and Fujiyama, 2002). A third isoform, VGLUT3, is distributed in subsets of neurons across the cortex, hippocampus, and striatum, but appears to have a more complex role in glutamatergic transport and synaptic activity (Fremeau et al, 2002; Gras et al, 2002; Herzog et al, 2004; Schäfer et al, 2002; Seal and Edwards, 2006). In order to further elucidate the role of VGLUTs in visual projections and the relative distributions of VGLUT isoforms in visual areas, we examined the mRNA and protein distributions of VGLUT1 and VGLUT2 in select subcortical nuclei and cortical visual areas of macaque monkeys. We find that VGLUT1 and VGLUT2 characterize distinct types of visual projections; VGLUT2 predominates in relay or feedforward projections from hierarchical lower order to higher order levels of the visual system, while VGLUT1 appears in modulatory connections within and between visual areas, as well as feedback connections from higher order to lower order structures. Since VGLUT1 and VGLUT2 are known to characterize distinct types of glutamatergic synapses in the central nervous system and

regulate differential rates of glutamate release in neurons (Fremeau, 2004), we can conclude that these isoforms also define separate glutamatergic projections at the level of neuronal circuits as well. Thus, VGLUT1 and VGLUT2 may define distinct types of excitatory projections within the primate visual system.

2. Materials and Methods

Four adult macaque monkeys *(Macaca fascicularis)* were used in this study. All procedures were approved by the Institutional Animal Care and Use Committee of Vanderbilt University and followed the guidelines mandated by the National Institutes of Health.

2.1 Tissue acquisition

One monkey was transcardially perfused with sterile 0.1M phosphate-buffered saline (PBS) followed by sterile 1% paraformaldehyde (PFA) in PBS at the University of Washington. The intact brain was removed and shipped overnight to Vanderbilt University, where the cortical hemispheres were bisected and separated from the thalamus and brainstem. One cortical hemisphere, as well as the thalamus and brainstem, were postfixed in sterile 4% PFA for 6 hours. The unfixed cortical hemisphere was used in an unrelated study. Following postfixation, pia was removed from the exterior surfaces, all pieces were blocked, and all blocks were cryoprotected in 30% sucrose for at least 24 hours prior to histology. The other three monkeys were overdosed with sodium pentobarbital (120mg/kg) and transcardially perfused with PBS followed by 4% PFA in PBS. The brains were removed and the cortical hemispheres were separated from the thalamus and brainstem. Two of the six cortical hemispheres were used in unrelated studies. The remaining hemispheres, as well as the thalamus and brainstem from all three animals, were blocked and cryoprotected in 30% sucrose for 24 hours prior to histology.

2.2 Histology

Cryoprotected blocks from each cortical hemisphere were cut on a sliding microtome into 40–50μm coronal sections and separated into alternating series for further study. Each series contained 50–70 sections distanced ~240μm apart in the brain. One series from each block was processed for cytochrome oxidase (CO; Wong-Riley 1979) and another series was processed for Nissl substance with thionin; both were used as references for architectonic boundaries of visual areas. Remaining series were cryoprotected (30% glycerol, 30% ethylene glycol, 0.1M PBS) and stored at −20°C for further use.

2.3 Immunohistochemistry (IHC)

Immunolabeling for VGLUT1 and VGLUT2 used commercial antibodies against each transporter (see Table 1 for details). Briefly, sections were postfixed for 30min in 4% PFA and rinsed in 0.01% Triton X-100 (Fisher, Pittsburgh PA) in 0.01M PBS. Endogenous peroxidase reactivity was quenched using 0.01% hydrogen peroxide in 0.01M PBS. Sections were rinsed again in 0.01% Triton/PBS, blocked in 5% normal serum (Vector Labs, Burlingame CA) and 0.05% Triton in 0.01M PBS for two hours, and then incubated overnight in the desired concentration of primary antibody (Table 1) with 5% serum and 0.05% Triton in 0.01M PBS. Two antibodies were used for VGLUT1 labeling to confirm the diffuse and variable staining pattern of VGLUT1 in all areas. Following primary incubation, sections were rinsed three times in 0.01% Triton/PBS, and then incubated in the desired secondary antibody with 5% serum and 0.05% Triton in PBS for two hours. Sections were rinsed three times in 0.01% Triton/PBS again, and then incubated in an avidin/biotinyl-peroxidase complex solution (ABC kit, Vector Labs) overnight. Sections were then rinsed three times in 0.01% Triton/PBS to remove nonspecific binding, and then incubated in 0.0002% 3’3’ diaminobenzidine with 0.02% nickel in 0.1M PBS to visualize the stain.

Sections were mounted on gelatin-subbed slides, dehydrated, and coverslipped with Permount (Fisher). Two series for each area were processed separately for VGLUT1 and VGLUT2 IHC.

2.4 Western Blotting (WB)

The specificity of each antibody used in VGLUT1 and VGLUT2 IHC was confirmed using standard western blotting techniques. Prior to perfusion, macaque cerebellar tissue was collected and placed in lysis buffer (0.32M sucrose, 2mM EDTA, 1% sodium dodecyl sulfate, 1ug/ml Leupeptin, 50um phenylmethylsulfonyl fluoride, Roche Complete protease inhibitors; Roche) on ice for 10 minutes. Tissue was homogenized using a Kontes pellet pestle (VWR, Radnor PA) and centrifuged at 1700g for 10 minutes. Supernatant was collected from each sample, total protein concentration was determined using a bicinchoninic acid assay kit (Pierce, Rockford IL), and all samples were normalized to 1ug/ul. Roughly 20–40ug of total protein was separated using SDS-PAGE and transferred to PVDF blotting membranes (Roche) overnight. Membranes were rinsed in 0.1M Tris-buffered saline (pH 8.0; Sigma) with 0.01% Triton, blocked in 5% bovine serum albumin (BSA, Roche) with 0.01% Triton for one hour, and then incubated overnight in the desired primary antibody (see Table 1 for details) with 5% BSA and 0.01% Triton, at 4°C with gentle agitation. Following primary incubation, membranes were rinsed in TBS/Triton and incubated in the desired horseradish peroxidase (HRP)-conjugated secondary antibody with 5% BSA and 0.01% Triton for one hour. Membranes were rinsed several times in TBS/Triton to remove background reactivity and labeled protein on each membrane was visualized using chemiluminescence and exposure to film. Film exposures for each western blot were scanned using a digital scanner and converted to digital images.

2.5 In situ hybridization (ISH)

Digoxigenin-labeled riboprobes for *VGLUT1* and *VGLUT2* mRNA were prepared from macaque cDNA libraries under previously described conditions (Tochitani et al, 2001) and labeled using a conventional DIG-dUTP labeling kit (Roche). ISH was performed with slight modifications of previously described techniques. All sections were postfixed overnight in 4% PFA, incubated in 0.75% glycine for 15 minutes to remove background reactivity due to formaldehyde fixation, and then incubated in 0.3% Triton for 15 minutes to increase permeability. Sections were treated with 0.1% Proteinase K (Sigma) for 30 minutes at 37°C, excess Proteinase K was acetylated using 0.25% acetic anhydride in 0.9% triethanolamine and 0.12% hydrochloric acid for 10 minutes, and all sections were preincubated in hybridization buffer (pH 7.5) containing 5% saline sodium citrate (SSC; 150 mM sodium chloride, 15 mM sodium citrate, pH 7.0), 50% formamide (FA), 2% blocking reagent (Roche), 0.1% N-lauroylsarcosine (NLS), 0.1% sodium dodecyl sulphate (SDS), and 20 mM maleic acid for one hour at 60°C. Sections were then hybridized overnight at 60°C in the same buffer, along with 1ug/ml of the desired probe. Hybridized sections were treated with 20 μg/mL RNase A (Sigma) in RNase A buffer (10 mM Tris-HCl, 10 mM ethylenediamine-N,N,N′,N′ -tetraacetic acid (EDTA), 500 mM NaCl; pH 8.0) for 15 minutes at 37°C to remove nonspecific mRNA. Finally, sections were thoroughly rinsed in Tris-buffered saline (pH 7.5; Sigma) for 15 minutes, blocked in 0.5% blocking reagent (Roche) for 30 minutes, and incubated with an alkaline phosphatase labeled anti-DIG antibody (1:1000, Roche) in 0.5% blocking reagent for four hours. Sections were then visualized overnight with 1:50 NBT/BCIP (Roche) in Tris 9.5, mounted on gelatin-subbed slides, dehydrated in ethanol and cleared in xylene, and coverslipped with Permount. Two series for each area were processed separately for *VGLUT1* and *VGLUT2* ISH.

2.6 Imaging and analysis

Digital photomicrographs and montages were captured using an MBF CX9000 camera mounted on a Nikon E80i microscope with Neurolucida software (MBF Bioscience, Williston, VT). All images were cropped and adjusted for brightness and contrast, but were otherwise unaltered.

3. Results

Protein and mRNA distributions of VGLUT1 and VGLUT2 varied significantly between and within visual structures, but remained largely consistent with known VGLUT distributions in other primate species (Balaram et al, 2011a, b; Garcia-Marin et al, 2013; Hackett et al, 2009). We find that VGLUT1 and VGLUT2 appear to characterize distinct types of glutamatergic projections within the macaque visual system. *VGLUT1* mRNA was moderately expressed in the lateral geniculate nucleus and pulvinar complex but strongly expressed in V1 (area 17) and V2 (area 18). *VGLUT2* mRNA, in contrast, was strongly expressed in the lateral geniculate nucleus, discrete layers of the superior colliculus, and the pulvinar complex, but only moderately expressed in certain layers of V1 and V2. VGLUT1 and VGLUT2 protein labeling was restricted to axon terminals in all areas examined, with the exception of a few cells in the pulvinar complex. VGLUT1 protein was diffusely expressed in all visual structures, and the intensity of labeling varied between and within regions of interest. VGLUT2 protein however, was localized to retinorecipient regions of the lateral geniculate nucleus and superior colliculus and tectorecipient divisions of the pulvinar complex, as well as specific layers of V1 and V2. The detailed distributions of VGLUT1 and VGLUT2 are discussed below.

3.1 Specificity controls for VGLUT1 and VGLUT2

In situ hybridization using sense and antisense probe strands against *VGLUT1* and *VGLUT2* mRNA confirmed the specificity of both probes to their respective RNA targets, with no crossreactivity between sequences and no detectable background reactivity, in macaque brain tissue (figure 1A–B). Western blots for all antibodies against VGLUT1 and VGLUT2 protein also showed strong specificity with no detectable background immunoreactivity in macaque cerebellar tissue (figure 1C). VGLUT1 was localized at 73kDa and VGLUT2 was localized at 56kDA, consistent with known molecular weights of both proteins. The rabbit polyclonal antibody against VGLUT1 labeled a portion of the full VGLUT1 protein (65kDa), as noted by the manufacturer, but comparisons of staining distributions confirm that both VGLUT1 antibodies label the correct protein (data not shown). Additionally, no differences in staining intensity were noted between sections from animals perfused with 1% PFA or 4% PFA. These findings demonstrate the specificity of the antibodies to VGLUT1 and VGLUT2, and eliminate concerns about nonspecific selectivity of the chosen probes and antibodies in macaque tissue.

3.2 Subcortical distributions of VGLUT1 and VGLUT2

VGLUT1 protein was densely and evenly distributed across the lateral geniculate nucleus, superior colliculus, and pulvinar complex while VGLUT2 protein was confined to more discrete distributions such as the retinorecipient layers of the lateral geniculate nucleus and superior colliculus, and tectorecipient regions of the inferior pulvinar. In all three subcortical areas, *VGLUT1* mRNA was expressed at low levels while *VGLUT2* mRNA was expressed at high levels, and both mRNA distributions correlated with known projections from these structures. Differences in VGLUT distributions in subcortical visual areas appear to identify distinct afferent and efferent projections from each area, as detailed below.

3.2.1 Superior Colliculus (SC)—The superior colliculus in macaques is a large, well-laminated midbrain structure that is traditionally divided into superficial, intermediate, and deep sets of layers, each of which mediates different functions within the SC (May, 2006). The majority of visual processing in the SC occurs in the superficial layers, while the deep layers regulate multisensory integration and brainstem motor functions. For the purposes of this study, only the superficial layers are considered. The most superficial layer of the SC is the stratum zonale or zonal layer (SZ), a narrow band of axon fibers that covers the dorsal surface of the colliculus. Just ventral to the SZ lies the stratum griseum superficiale or superficial gray layer (SGS), an intermediately sized, cell dense layer that can be divided into upper and lower subdivisions (uSGS and lSGS, respectively) in most primates. Ventral to the SGS lies the stratum opticum or optic layer (SO), similar in size to the SGS but largely cell free and instead filled with fiber tracts that run lateral to medial through the layer. Laminar divisions of the superior colliculus are indicated in figure 2.

In Nissl preparations of the superior colliculus (figure 2A), the SZ was distinguishable as two layers across the dorsal surface of the colliculus, the upper layer consisting of a thin row of cells of mostly astrocytes (Lund 1972), and a lower layer of fibers that cross the extent of the SC. The SGS was also visible below the SZ, and could be separated into upper and lower subdivisions based on cell density. The SO showed much sparser cell distributions than the overlying layers of the SC. In CO preparations (figure 2B), the upper SZ stained weakly for CO and appeared as a light band across the surface of the colliculus, while the lower SZ stained strongly for CO and appeared as a thin, dark band. The SGS could also be differentiated into its respective subdivisions, the upper SGS showed dense CO staining while the lower SGS showed more moderate CO reactivity. The SO stained lightly for CO, mostly between the fiber tracts running through this layer, appearing as a light, medium-sized band that originated from the optic tract on the lateral edge and continued to the medial aspect of the SC. From rostral to caudal sections in the colliculus, the SZ remained a uniform size while the SGS and SO appeared to decrease in relative thickness. No cells were visible in CO-stained sections of the SC. With the exception of upper and lower subdivisions of the SZ in CO preparations, both Nissl and CO distributions in the macaque SC are consistent with previous descriptions of lamination in the primate colliculus (May 2006).

The labeling of VGLUT1 and VGLUT2 protein in the superficial layers of the SC likely reflects retinotectal and corticotectal terminal projections (Symonds and Kaas, 1978; Tigges and Tigges, 1970; figures 2C–D, 3A–B). VGLUT1 was densely distributed across all the superficial layers of the SC, indicating its considerable use in retinal or cortical projections (figures 2C, 3A). The SZ was discernible as two bands; the upper astrocytic layer was devoid of VGLUT1 and the lower fiber layer was densely labeled with VGLUT1. The SGS was also clearly split into two divisions; the upper SGS stained darkly for VGLUT1 and the lower SGS stained more moderately for VGLUT1. The SO showed even, diffuse labeling of VGLUT1 throughout the SC, mostly apparent as punctate labeling around the fibers running through this layer. No differences in VGLUT1 labeling were seen between rostral and caudal extents of the SC. In contrast, VGLUT2 labeling in the SC was concentrated in the lower SZ and dorsal parts of the upper SGS, appearing as dense, regular patches of label through the rostrocaudal extent of the colliculus (figures 2D, 3B). VGLUT2 labeling in the lower SZ/upper SGS was consistently denser along the medial aspect compared to the lateral aspect of the SC. Moderate VGLUT2 terminal labeling was observed through the rest of the SGS and SO, but remained at reduced levels through the colliculus. The discrete, patchy labeling of VGLUT2 terminals seen in the superficial layers of the SC closely resembles previous descriptions of retinotectal terminations in macaques (Hubel et al, 1975; Pollack and Hickey, 1979; Wilson and Joyne, 1970) while the diffuse, even labeling of VGLUT1 terminals more resembles patterns of corticotectal terminations (Wilson and Joyne, 1970).

Thus, VGLUT1 and VGLUT2 likely characterize the terminations of distinct visual projections to the macaque SC.

Tectopulvinar and tectogeniculate projection neurons were examined using *VGLUT* mRNA expression, which identified *VGLUT1* or *VGLUT2* mRNA-positive cells in the SC that utilize the respective protein in their axon terminals (figures 2E–F, 3C–D). *VGLUT1* mRNA was notably absent from all superficial layers of the SC (figures 2E, 3C). A few large *VGLUT1*-positive neurons were found in the intermediate layers and along the edge of the periaqueductal gray, confirming the reaction technique, but similarly stained cells were not found in the SZ, SGS or SO, indicating that efferent projections from the SC do not appear to utilize *VGLUT1* for excitatory transmission. *VGLUT2* mRNA however, was differentially distributed throughout the superficial layers of the SC (figures 2F, 3D). Both layers of the SZ and the upper SGS were devoid of *VGLUT2* mRNA, but the lower SGS contained numerous medium-sized cells that stained strongly for *VGLUT2.* In caudal sections of the SC, *VGLUT2*-positive cells in the lower SGS were evenly distributed from the medial to lateral edge, but in more rostral sections they were concentrated along the lateral aspect of the SC. The SO contained a scattered distribution of smaller and more moderately stained *VGLUT2*-positive cells. Cells in the lower SGS of the colliculus project to specific divisions of the inferior pulvinar in macaques (Stepniewska et al, 2000) and strong *VGLUT2* mRNA expression in this layer corresponds to strong VGLUT2 terminal labeling in those divisions of the pulvinar complex (discussed below).

3.2.2 Pulvinar—The primate pulvinar is a large complex of several nuclei within the thalamus that are well connected to a number of visual and nonvisual cortical areas, with some nuclei also receiving inputs from the SC (Stepniewska, 2004). The pulvinar of macaques has been traditionally subdivided into four major regions; the anterior pulvinar (PA), the medial pulvinar (PM), lateral pulvinar (PL), and inferior pulvinar (PI). PI in macaques has been subdivided into four areas, posterior inferior pulvinar (PIp), medial inferior pulvinar (PIm), and central inferior pulvinar (PIc), which was further subdivided into medial and lateral divisions, PIcm and PIcl respectively (Stepniewska et al, 1997). While the traditional boundary between PI and PL and PM has been the brachium of the superior colliculus, all subdivisions of PI continue into the ventral portions of PM and PL. PA is not connected to occipital and other visual areas that contribute to early stages of visual processing, and thus, is not discussed here. PM, PL, and PI however, are connected with various cortical visual areas and likely serve a crucial role in processing and integrating visual information. Subdivisions of the pulvinar complex in macaques are shown in figure 4.

Nissl preparations through the pulvinar complex (figure 4A) clearly distinguished the three major pulvinar subdivisions as previously described (Olszewski 1952). Nissl stained cells in PM were densely packed and evenly distributed, while cells in PL were irregularly distributed between fiber bundles running lateral to medial through the nucleus. PI could be separated into three divisions based on cell density; PIm showed dense cell distributions, clearly distinguishing it from the more diffuse cell distributions of PIp and PIc. CO-stained sections through the pulvinar better delineated the subdivisions of this area (figure 4B); PM showed moderate CO reactivity with multiple darker patches along the ventrolateral aspect that were continuous with subdivisions of PI, while PL showed more irregular CO reactivity with light and dark areas dispersed between fiber bundles. PI could be divided into four regions; PIm stained strongly for CO, distinguishing it from PIp and PIcm, both of which stained weakly for CO. PIcl showed slightly stronger CO reactivity than PIcm in rostral and middle sections through the pulvinar complex. Previous CO descriptions of the macaque pulvinar identified similar patterns as those described above (Stepniewska 1997, 2000, 2004), providing us with consistent definitions of boundaries between pulvinar divisions.

Afferent terminations in the pulvinar complex were largely characterized by dense, even distributions of VGLUT1 and not VGLUT2 (figures 4C–D, 5A–L). PM showed dark, punctate staining of VGLUT1 across its extent (figure 4C, 5A–F), with slightly darker labeling along the dorsomedial boundary of PM (best seen in figure 4C). PL showed more diffuse VGLUT1 reactivity dispersed between the brachial fiber bundles (figure 5B). PI could be separated into four divisions; PIp and PIcm stained less darkly for VGLUT1, with small punctate terminals distributed throughout both structures (figure 5C, E), and appeared as lighter bands around PIm (best seen in figure 4C). Labeled terminals in PIm appeared much smaller than those seen in PIp and PIcm, and diffuse neuropil labeling of VGLUT1 was also apparent in this region (figure 5D). Lastly, VGLUT1 staining in PIcl closely resembled that of PL (figure 5F), with diffuse terminal labeling distributed through the region. In contrast to VGLUT1, strong VGLUT2 reactivity was only found in two subdivisions of the pulvinar complex, PIp and PIcm (figures 4D, 5G–L), Both regions showed dense, patchy distributions of VGLUT2 positive terminals (figure 5I, K), while all other pulvinar divisions showed weak cellular labeling of VGLUT2. Strong labeling of VGLUT2 positive terminals in PIcm and PIp also continued dorsal and ventral to PIm in most sections (figure 4D), suggesting that these two regions of dense VGLUT2 labeling are parts of the same nucleus. Diffuse cellular labeling of VGLUT2 clearly distinguished PIm from the surrounding pulvinar, and differentiated PIcl from PIcm, but did not distinguish PM from PL. The diffuse labeling of VGLUT1 in all divisions of the pulvinar likely correspond to multiple cortical projections that terminate within this structure, while the discrete labeling of VGLUT2 terminals in PIp and PIcm correspond to subcortical projections from the lower SGS of the colliculus. Thus, VGLUT1 and VGLUT2 likely typify the synaptic terminations of distinct afferent projections within the pulvinar complex (Masterson et al, 2009).

Neurons within the pulvinar, which project to a variety of visual cortical areas, were disparately characterized by both *VGLUT1* and *VGLUT2* mRNA (figures 4E–F, 5M–X). VGLUT1 was only weakly expressed in scattered cells throughout the pulvinar complex, making it difficult to detect changes in *VGLUT1* expression between pulvinar divisions (figures 4E, 5M–R). *VGLUT2* mRNA was more strongly expressed in all divisions of the pulvinar, but expression patterns within often heterogeneous within each division (figures 4F, 5S–X). In general, PIp and PIcm showed similarly strong *VGLUT2* expression, with dense clusters of large and medium sized *VGLUT2* positive cells (figure 5U, W). PL and PIcl also showed strong *VGLUT2* expression, in smaller cells that were closely packed (figure 5T, X). Lastly, PM and PIm showed weak levels of *VGLUT2* expression in a small percentage of cells within each division (figure 5S, V). The distinct patterns of *VGLUT1* and *VGLUT2* mRNA highlight the heterogeneity of glutamatergic projection neurons within the pulvinar complex.

3.2.3 Lateral Geniculate Nucleus (LGN)—The dorsal lateral geniculate nucleus in macaques is composed of cell-dense layers, interleaved by cell-sparse interlaminar zones (figure 6). LGN layers are traditionally defined by their cell type and relative location within the nucleus; from ventral to dorsal, they are classified as external magnocellular (ME), internal magnocellular (MI), internal parvocellular (PI), and external parvocellular (PE). In macaques, both parvocellular layers split into alternating leaflets and appear as four layers instead of two (Kaas et al, 1978). Boundaries between LGN layers and interlaminar zones were easily distinguishable in CO and Nissl stained sections (figure 6A–B,) and were consistent with previous descriptions of this nucleus (Kaas et al, 1978).

Major afferent terminations in the LGN from the retina, superior colliculus, and primary visual cortex were labeled by staining for VGLUT1 and VGLUT2 protein. Sections stained for VGLUT1 showed dense but diffuse labeling of axon terminations through the M and P

layers, as well as the interlaminar zones of the LGN (figures 6C, 7A–C). The dorsal leaflet of PE appeared to stain darker for VGLUT1 compared to the other layers, across all sections of the LGN (best seen in figure 6C), but no other differences were noted in staining intensity between the layers. The interlaminar zones stained more diffusely for VGLUT1 and could be distinguished from neighboring LGN layers based on their reduced staining intensity. In comparison to VGLUT1, VGLUT2 distributions in the LGN were remarkably different; punctate terminal labeling of VGLUT2 was densely packed in the M and P layers but largely absent from the interlaminar zones (figures 6D, 7D–F). Stronger and denser VGLUT2 labeling was seen in the M layers in comparison to the P layers in all sections of the LGN (figures 6D, 7D). The discrete labeling of VGLUT2 terminals within the LGN layers matches patterns of retinogeniculate terminations in macaques (Conley and Fitzpatrick, 1989; Kaas et al, 1978) while the diffuse labeling of VGLUT1 terminals resemble cortical projections to this nucleus (Lund et al, 1975). Thus, VGLUT1 and VGLUT2 appear to resemble distinct projections within the macaque LGN.

LGN projection neurons were examined for *VGLUT* mRNA expression (figures 6E–F, 7G–L). *VGLUT1* mRNA was weakly expressed in cells of all LGN layers and interlaminar zones (figures 6E, 7G–I). In sections stained for *VGLUT2* mRNA, most cells in the M and P layers strongly expressed *VGLUT2,* while cells in the interlaminar zones did not (figures 6F, 7J–L). VGLUT2 positive cells in the P layers were more densely packed than those in the M layers, but no other laminar differences were found. Lastly, no rostrocaudal differences in *VGLUT1* and *VGLUT2* expression were seen in the LGN. Cells in the LGN primarily project to V1 (Hendrickson et al, 1978) and the dual expression of both *VGLUT1* and *VGLUT2* mRNA within the magnocellular and parvocellular LGN layers suggests that these cells use both isoforms in their cortical projections. Isolated *VGLUT1* expression in the koniocellular layers suggests that these cells use a single isoform in glutamatergic transmission instead.

3.3 Cortical distributions of VGLUT1 and VGLUT2

Large-scale differences were seen in VGLUT distributions between V1 and V2. Overall, *VGLUT1* mRNA predominated in cortical neurons while *VGLUT2* mRNA only identified a subset of neurons from these areas. Additionally, VGLUT1 protein was diffusely distributed in V1 and V2 while VGLUT2 was restricted to discrete terminations. The differential distribution of VGLUT isoforms in cortical areas again suggests that these proteins characterize separate glutamatergic projections in the macaque visual system.

3.1 Area V1

V1 in macaques is easily identified by its extensive lamination and distinct architectonic characteristics. Here, V1 layers and sublayers are numbered according to Hassler's (1967) scheme (figure 8B), rather than the more common scheme of Brodmann (1909), as evidence from numerous comparative and other studies support this classification (Casagrande and Kaas, 1994, for review). The primary difference between these schemes is their delineation of layer 4 in V1; Brodmann's scheme includes 3 sublayers of layer 4, 4A, 4B, and 4C, while Hassler's scheme labels Brodmann's 4A and 4B as sublayers of layer 3, 3B and 3C respectively, and Brodmann's layer 4C as a single layer 4. Subdivisions of all V1 layers in macaques are distinctly visible in Nissl stains that demarcate cell size and density in this area (figures 8C, 9A). The abrupt change in lamination between V1 and V2 also clearly marks the boundary between both areas (figure 8). CO stained sections through V1 revealed distinct patterns of lamination based on staining intensity (figure 8D, 9B). Layer 1 showed no reactivity, and layers 2, 3 and 5 stained lightly for CO. Layers 3bβ and layer 4 stained darkly for CO and appeared as distinct bands that terminated at the border between V1 and V2. Patches of strong CO reactivity were visible at regular intervals in layer 3, identifying

the blob and interblob compartments of V1 (Wong Riley, 1979). Lastly, layer 6 stained moderately for CO and appeared as another distinct band ventral to layer 5. CO and Nissl stains through V1 were consistent with previous reports, and provided a reliable basis of laminar and areal definitions in the macaque visual cortex (Casagrande and Kaas, 1994).

VGLUT protein distributions varied distinctly between the layers of V1 (figures 8E–F, 9C–D). Layers 1 and 3A stained densely for VGLUT1 but not VGLUT2. Layer 2 showed scattered populations of VGLUT2 positive terminals clustered towards to dorsal boundary of the layer (best seen in 8D), which resembled pulvinar terminations in V1 (Ogren and Hendrickson, 1977), and dense VGLUT1 reactivity throughout. Layers 3B and 3C stained weakly for both VGLUT proteins and appeared as lighter bands within the superficial layers of V1. Layer 3Bβ, however, showed unique staining patterns of both VGLUT isoforms; a thin band of strong VGLUT1 labeling and a thin band of strong VGLUT2 labeling were present, with the VGLUT1 band consistently dorsal to the VGLUT2 band throughout V1. When aligned with CO sections, both bands fell within the strong belt of CO reactivity seen in layer 3Bβ. Thus, two different types of VGLUT inputs are segregated within layer 3Bβ. Layer 4 also showed unique expression patterns of VGLUT1 and VGLUT2. Both 4A and 4B had dense distributions of VGLUT1 and VGLUT2 compared to the other layers of V1, but the densest labeling of VGLUT1 appeared at the border between 4A and 4B while the densest labeling of VGLUT2 appeared in 4B proper. Alignment with CO sections confirmed that both dense VGLUT bands were within layer 4. Layer 5 labeled weakly for VGLUT1 and VGLUT2, while layer 6 exhibited more moderate labeling of both proteins. With the exception of 6A, which had slightly stronger VGLUT1 staining than 6B, neither layer 5 nor layer 6 presented any sublaminar differences in VGLUT reactivity. The distinctive laminar distributions of VGLUT1 and VGLUT2 proteins ended at the border between V1 and V2 (figure 8E,F), indicating that these patterns are unique to V1.

Dense VGLUT2 labeling in layer 4A, 4B and 3Bβ likely reflects magnocellular and parvocellular geniculostriate input to V1 (Hendrickson et al, 1978), as evidenced by strong VGLUT2 mRNA expression in those layers of the LGN. The dorsal band of VGLUT1 labeling in layer 3Bβ, as well as dense VGLUT1 labeling at the 4A/4B border, llikely reflects a distinct subset of parvocellular geniculate inputs to V1 (Hendrickson etal, 1978), and corresponds to the expression of *VGLUT1* mRNA in those LGN layers as well. Alternatively, but less likely given the weak levels of *VGLUT1* mRNA seen the cell bodies of these projections, the bands of VGLUT1 labeling in V1 could correspond to koniocellular geniculate terminations in layer 3Bβ (Lund, 1988).

Neurons that expressed *VGLUT1* and *VGLUT2* mRNA were found in discrete layers of V1 (figures 8G–H, 9E–F). Layer 1 did not express either VGLUT isoform, consistent with its very sparse distribution of neurons. Layers 2 and 3A showed dense expression of *VGLUT1* and weak expression of *VGLUT2.* In both layers, labeled cells were small and densely packed. Sublayers 3B and 3Bβ were slightly more heterogeneous in expression patterns and cellular distributions; both layers contained small, medium, and large cells interspersed with each other, some cells with strong *VGLUT1* or *VGLUT2* expression and others with more moderate labeling, making it difficult to determine consistent expression patterns within these layers. In general, it appeared that larger cells stained darkly for *VGLUT2* while smaller cells stained darkly for *VGLUT1,* although quantification would be needed to support this conclusion. Layer 3C exhibited distinct differences in *VGLUT* distributions; while neither *VGLUT* isoform was particularly predominant in 3C, *VGLUT1* positive cells tended to cluster towards the dorsal and ventral edges of layer 3C while *VGLUT2* positive cells were evenly distributed through the center of the layer. No differences in labeled cell size or density were observed in 3C. In layer 4, medium-sized cells throughout 4A and 4B moderately expressed *VGLUT2,* while much smaller cells in both layers weakly expressed

VGLUT1. On average, *VGLUT2* positive cells in 4A were larger, darkly stained, and more frequently distributed than *VGLUT2* positive cells in 4B, which were lightly stained but densely packed. *VGLUT1* positive cells in 4A and 4B showed equal levels of expression, but cells in 4B were again crowded together compared to 4A. Layer 5 of V1 contained weak *VGLUT1* expression in small cells but no *VGLUT2* expression; in general, *VGLUT1* positive cells in 5A were clustered together compared to *VGLUT1* positive cells in 5B. In contrast, layer 6A showed strong *VGLUT1* expression while 6B showed weaker *VGLUT1* expression, clearly distinguishing them through the extent of V1. Some cells in layer 6 stained weakly for *VGLUT2* but could not be reliably identified throughout the area. Overall, *VGLUT1* and *VGLUT2* mRNA expression overlapped significantly in the superficial layers, but varied distinctly in layer 4 and the deep layers of V1.

3.2 Area V2

V2 in macaques covers a thin strip of the cortical surface along the full extent of the anterior border of V1 (DeYoe and Van Essen, 1985; Kaas, 2005). Like V1, it contains a topographic map of the contralateral visual field across its surface. In coronal sections through the occipital cortex, V2 is identified by its distinct border with V1. Nissl stains in coronal sections of V2 reveal its laminar characteristics, most notably a thin, cell dense layer 4 and a broad layer 3 that can be subdivided into three layers based on relative cell density (figures 8C, 10A). CO staining in coronal sections of V2 reveals fewer distinct characteristics; ventral parts of layer 3 and dorsal parts of layer 4 showed slightly stronger CO reactivity, but the remaining layers show uniform CO staining across V2 (figures 8D, 10B). Since the rostral border of V2 is relatively ambiguous in coronal sections stained for Nissl and CO, VGLUT distributions aligned to these stains were largely analyzed from caudal regions in V2, near the border of V1.

Overall, VGLUT protein distributions in V2 were remarkably homogeneous, making it difficult to identify distinct laminar patterns in this area. However, general differences in staining intensity were observed (figures 8E,F and 10C,D). Layers 1, 2 and 3 stained strongly for VGLUT1 and weakly for VGLUT2, appearing almost continuous through the extent of V2. Layer 4 contained strong VGLUT2 reactivity, which resembled patterns of pulvinar terminations in V2 (Levitt et al, 1995; Marion et al, 2012, Ogren and Hendrickson, 1977) but relatively weak VGLUT1 staining throughout V2. Layer 5 showed slightly weaker VGLUT1 labeling than layer 4, and diffuse labeling of VGLUT2. Numerous darkly stained cell bodies were seen throughout layers 5 and 6 in VGLUT2 preparations (best seen in figure 8F). Layer 6 also stained moderately for VGLUT1, identifying it as a distinct band along the ventral edge of V2 (figure 10C). Just as in V1, VGLUT1 and VGLUT2 distributions largely overlap in the superficial layers but become more distinct in the middle and deep layers of V2.

Neurons expressing *VGLUT1* or *VGLUT2* mRNA revealed laminar patterns in V2 (figures 8G,H and 10E,F). Layer 1 again did not express either isoform, and layer 2 weakly expressed both *VGLUT1* and *VGLUT2* in small, densely packed cells. Layer 3 could be differentiated into three sublaminae based on VGLUT expression. The dorsal sublayer, 3A, strongly expressed *VGLUT1* and moderately expressed *VGLUT2; VGLUT1* positive cells were both medium or small in size and evenly interspersed within 3A, while *VGLUT2* positive cells were small and diffusely spread through the layer. The middle sublayer, 3B, showed moderate *VGLUT1* expression and sparse *VGLUT2* expression; *VGLUT1* positive cells were smaller compared to cells in the other sublayers, but more densely packed. The ventral sublayer, 3C, strongly expressed both *VGLUT1* and *VGLUT2; VGLUT1* positive cells ranged in size but were evenly distributed in 3C, while *VGLUT2* positive cells were large but scattered unevenly through the layer. Layers 4, 5 and 6 all strongly expressed *VGLUT1* but did not express *VGLUT2. VGLUT1* positive cells were small and densely

packed in layer 4, large and diffusely spread in layer 5, and large or medium in size but more condensed in layer 6. Similar to patterns seen in V1, *VGLUT1* and *VGLUT2* expression overlapped to some extent in the superficial layers of V2, but varied distinctly in the middle and deep layers ofV2.

4. Discussion

The present study examined the distribution patterns of VGLUT1 and VGLUT2 mRNA and protein in cortical and subcortical structures of the macaque visual system. The specific distributions of VGLUT1 and VGLUT2 were informative in two ways; first, discrete patterns of VGLUT mRNA and protein allowed us to identify subdivisions of visual cortical areas and subcortical nuclei; second, the distributions of VGLUT1 and VGLUT2 in visual pathways correlate with cortical and subcortical circuits that have been defined as driving or modulatory connections between visual areas and nuclei. Thus, VGLUT1 and VGLUT2 usefully define subdivisions of visual structures, and they appear to characterize driving and modulatory inputs at different levels of the macaque visual system. A detailed analysis of our results with respect to these two conclusions follows below.

4.1 VGLUT1 and VGLUT2 identify functional subdivisions of subcortical and cortical visual structures in macaque monkeys

Architectonic boundaries between and within visual cortical areas and subcortical nuclei were clearly visible in VGLUT1 and VGLUT2 preparations. Distinct patterns of VGLUT1 and VGLUT2 terminal labeling distinguished previously defined layers of the superior colliculus, lateral geniculate nucleus, V1 and V2, as well as subdivisions of the inferior pulvinar, while distributions of cells expressing *VGLUT1* or *VGLUT2* mRNA also identified the laminar or regional origins of glutamatergic projections from each structure.

Laminar divisions of the superior colliculus were clearly demarcated in VGLUT preparations. Dense, patchy VGLUT2 terminal labeling identified the superficial gray layers where retinal projections terminate (figures 2D, 3B; Hubel et al, 1975; Pollack and Hickey, 1979), while diffuse VGLUT1 terminal labeling identified the laminar extent of corticotectal projections through the superficial gray layers that largely terminate at the boundary of the optic layer (figures 2C, 3A; Fries, 1984; Lock et al, 2003; Lund, 1972; Maunsell and Van Essen, 1983; May, 2006). The distribution of cells expressing *VGLUT2* mRNA also distinguished the extent of the lower superficial gray layer (figures 2F, 3D); these cells project to the posterior and central medial divisions of the inferior pulvinar (figure 11; Benevento and Fallon, 1975; Benevento and Standage, 1983; Harting et al, 1980; Stepniewska et al, 2000; Trojanowski and Jacobson, 1975) and their terminations were identified by dense VGLUT2 labeling in both inferior pulvinar divisions.

VGLUT distributions in the lateral and inferior pulvinar highlighted the heterogeneity of afferent and efferent projections in these nuclei, but were still instrumental in defining subdivisions in the inferior pulvinar. Diffuse VGLUT1 terminal labeling across the lateral and inferior pulvinar that resembled patterns of corticopulvinar terminations in macaques (Campos-Ortega and Hayhow, 1972; Maunsell and Van Essen, 1983; Ogren and Hendrickson, 1979) supports the conclusion that these structures are dominated by inputs from visual cortical areas and not subcortical structures (Adams et al, 2000; Bender, 1983; Shipp 2001; Van Essen 2005). Clear exceptions to this inference are the posterior and central medial nuclei of the inferior pulvinar, which primarily receive inputs from the superior colliculus (see above) and showed dense distributions of VGLUT2 positive terminals instead. Significant differences in the extent and localization of architectonic divisions within the inferior pulvinar have been reported in previous studies of Old World and New World primates (Stepniewska et al, 2000 for discussion), but four subdivisions of

PI have been consistently identified across primates (Cusick et al, 1993; Gutierrez et al, 1995; Lin and Kaas 1979; Stepniewska et al, 2000); the posterior inferior pulvinar (PIp), medial inferior pulvinar (PIm), central medial inferior pulvinar (PIcm) and central lateral inferior pulvinar (PIcl). PIcm and PIcl were originally considered a single nucleus until histological preparations identified them as distinct subdivisions (Stepniewska et al, 1997), and some studies suggest that PIp and PIcm were originally a single nucleus that was later divided by the evolution and intrusion of PIm into this area. Thus, PIp and PIcm often appear "bridged" or adjoined dorsally and ventrally around PIm in coronal histological preparations through the inferior pulvinar (for example, figures 12–14 in Stepniewska et al, 2000). VGLUT1 and VGLUT2 distributions clearly identified three distinct subdivisions of the inferior pulvinar that are spatially organized to form four regions within this structure (figure 4). The remarkable similarity in size, density, and *VGLUT* mRNA expression of cells in PIp and PIcm suggest that these two regions are functionally related but separated parts of the same nucleus, as previously proposed (Baldwin et al, 2012; Stepniewska et al, 2000; Symonds and Kaas, 1978). The continuation of VGLUT2 terminal labeling both dorsal and ventral to PIm also resembles the bridged pattern seen in previous histological preparations (Stepniewska et al, 1997) and supports the conclusion that PIp and PIcm were originally a single nucleus that have since separated and evolved distinct functions and connections (Baldwin et al, 2012; Cusick et al, 1993). PIm, which did not express *VGLUT1* or *VGLUT2* mRNA, and only showed dense labeling of VGLUT1 protein, could also be identified as a distinct subdivision between PIp and PIcm. PIcl, along the lateral most edge of the inferior pulvinar, could not be distinctly divided from PIcm, but general differences in cell size, density, and levels of *VGLUT* mRNA suggest that these regions are indeed distinct subdivisions of the inferior pulvinar. Thus, three anatomically distinct regions, PIcl, PIm, and PIcm-PIp, could be identified in VGLUT preparations and coincided with the spatial arrangement of four divisions seen in previous reports of the inferior pulvinar. Further studies of VGLUT expression in the inferior pulvinar of other mammals will undoubtedly help identify homologous subdivisions, leading to more consistent descriptions of the inferior pulvinar across species.

VGLUT distributions identified laminar divisions and the extent of visual projections within the lateral geniculate nucleus (figures 6, 7; Casagrande et al, 2006 for review). Strong *VGLUT2* expression in geniculostriate projection neurons clearly delineated the boundaries of magnocellular and parvocellular layers within the LGN while weak *VGLUT1* expression also identified koniocellular cells in the interlaminar zones. Discrete VGLUT2 positive terminal labeling also identified the extent of retinogeniculate projections, while diffuse VGLUT1 positive labeling identified the extent of corticogeniculate projections in this nucleus.

VGLUT preparations were also instrumental in defining laminar boundaries within cortical visual areas V1 and V2. Differences in cell size, density, and levels of *VGLUT* mRNA expression distinguished laminar boundaries in both visual areas, while distinct patterns of VGLUT1 and VGLUT2 terminal labeling identified afferent and efferent projections to these areas (DeYoe and Van Essen, 1985; Levitt et al, 1995; Lund, 1988; Sincich et al, 2010). Most notably, two different depths of terminations were noted for parvocellular geniculate projections to V1; a dorsal band of dense, VGLUT1-positive terminals along the 4A/4B border and a ventral band of equally dense, VGLUT2-positive terminals within layer 4B, neither of which overlap with the zone of magnocellular geniculate terminations in layer 4A of V1 (Lund et al, 1988). The significance of these distinct terminations is underscored by the expression of both *VGLUT1* and *VGLUT2* mRNAs in parvocellular cells of the LGN; it suggests that the dual use of VGLUT isoforms in geniculate projections can give rise to distinct terminations and perhaps, separate functions in visual processing. Since cells in the LGN do project to several areas of visual cortex (Benevento and Yoshida, 1981;

Bullier and Kennedy, 1983; Sincich et al, 2004; Yukie and Iwai, 1981), it is possible that geniculate projections differentially utilize VGLUT1 and VGLUT2 in their terminations across cortical areas. Since VGLUT1 and VGLUT2 regulate different probabilities of glutamatergic transmission (Fremeau et al, 2004, for review), these distinct terminations may contribute different valences of glutamatergic input to cortical areas in the macaque visual system.

4.2 VGLUT1 and VGLUT2 distinguish between driving and modulating visual projections

The distinct distributions of VGLUT1 and VGLUT2 in connections between visual structures suggest that these isoforms characterize separate types of glutamatergic projections. Previous studies have proposed that VGLUT1 characterizes corticothalamic projections while VGLUT2 characterizes thalamocortical projections (Barroso-Chinea et al, 2007; Fremeau et al, 2001; Fremeau, 2004; Graziano et al, 2008; Herzog et al, 2001), but recent work has shown more heterogeneous distributions of these isoforms in both cortical and subcortical projections (Balaram et al, 2012a, 2012b; Hackett et al, 2011; Ito et al, 2011; Masterson et al, 2009; Storace et al, 2012). With further examination of these distributions, and their correlation with previously reported functional properties of each projection (Crick and Koch, 1998; Felleman and Van Essen, 1981; Sherman, 2005; Sherman and Guillery, 1996, 2006, 2011; Van Essen, 2005;), we propose that VGLUT1 and VGLUT2 do characterize distinct types of glutamatergic projections; VGLUT2 predominates in feedforward or driving connections while VGLUT1 predominates in feedback or modulatory connections between visual structures. The visual projections evaluated in this study are outlined in figure 11.

The first major glutamatergic projection in the macaque visual system consists of retinal projections to all layers of the LGN as well as the superficial layers of the SC. These projections are considered driving or feedforward connections from sensory afferents (Sherman and Guillery, 1996), and were characterized by dense VGLUT2 terminal labeling in the retinorecipient layers of both structures. The next major visual projection, the geniculostriate pathway, arises from cells in all layers of the LGN and terminates in layers 3Bβ and 4 of V1 (Casagrande and Kaas, 1994 for review). Projections from the magnocellular and parvocellular geniculate layers are functionally considered driving or feedforward afferents (Sherman 2005; Sherman and Guillery, 1996, 1998;) and both projections are dominated by VGLUT2. While both geniculate cell types expressed low levels of *VGLUT1* mRNA as well, a characteristic of sensory relay nuclei (Balaram et al, 2012; Barroso-Chinea et al, 2007; Fremeau et al, 2001; Herzog et al, 2001; Ito and Oliver, 2010; Storace et al, 2012), these cells send branched afferents to multiple layers in V1 and the use of both VGLUT isoforms in their terminals may give rise to difference valences of driving and modulatory visual input to this area, as described above. Koniocellular cells in the LGN exclusively expressed *VGLUT1* mRNA, and these cells project to several visual cortical areas (Casagrande 2006; Sincich et al, 2004; Stepniewska et al, 1999) as well as several layers of V1 (Casagrande et al, 2007,) and have more of a modulatory role in geniculostriate visual processing (Casagrande, 1994; Casagrande and Norton, 1991; Kaas and Huerta, 1988). Feedback projections from V1 to the LGN, which primarily modulate visual signals passing through this nucleus (Sherman and Guillery 1996, 1998), arise in layer 6 of V1 and terminate diffusely across all layers of the LGN. Cells in layer 6 of V1 exclusively expressed *VGLUT1* mRNA, which corresponded to the diffuse VGLUT1 terminal labeling resembling corticogeniculate projections that was seen throughout the LGN. Thus, VGLUT1 and VGLUT2 appear to characterize modulatory and driving connections throughout the geniculostriate pathway of the macaque visual system.

Another glutamatergic projection, from the lower superficial gray layer of the superior colliculus to the posterior and central medial divisions of the pulvinar, exhibits several

characteristics of a driving or feedforward projection (Berman and Wurtz, 2010; Marrocco et al, 1981; Partlow et al, 1977). Strong *VGLUT2* expression in tectal neurons of the lower SGS corresponding to VGLUT2 terminal labeling in the lateral and central medial divisions of PI indicates that this projection also preferentially utilizes VGLUT2 for glutamatergic transmission. Cells in the tectorecipient regions of the pulvinar project to visual areas of temporal cortex that may play a role in blindsight (Poppel et al, 1985; Stoerig and Cowey, 2007; Tamietto et al, 2010) and predominant *VGLUT2* expression in these cells suggests that this driving projection preferentially utilizes VGLUT2 as well. While the upper superficial gray layer in the colliculus does have excitatory connections with the interlaminar zones of the LGN, the specific neurotransmitter used in these projections has yet to be identified in any species (Bickford et al, 2000) and tectogeniculate projections may have more of a modulatory role in visual processing given their specific terminations on koniocellular cells of the LGN (see above, Casagrande, 1994; Harting et al, 1978). Feedback projections to the superior colliculus arise in layers 5 and 6 of V1 and layer 6 of V2, in addition to projections from other cortical areas (Fries, 1984), and the dense expression of *VGLUT1* mRNA in these cortical layers corresponded to diffuse VGLUT1 terminal labeling seen across the superficial layers of the SC.

Feedforward or driving projections from V1 arise in layer 3, which projects to V2 and MT, and in layer 5, which projects to the lateral and inferior pulvinar (Casagrande and Kaas, 1994; Felleman and Van Essen, 1981; Sherman, 2005, 2012; Sherman and Guillery, 1998). The majority of smaller cells in the superficial layers of V1 express both *VGLUT1* and *VGLUT2* and likely give rise to both driving and modulatory connections depending on their intrinsic or extrinsic projections, as well as the context of transmitted information (Sherman and Guillery, 2004). However, large pyramidal neurons that only expressed *VGLUT2* were largely confined to layers 3C and 5A, which primarily project to MT and the pulvinar respectively. Layer 4 of MT, where V1 projections terminate, showed dense distributions of VGLUT2 positive terminals as well. Layer 4 of V2, which is the primary recipient of feedforward projections from the lateral and inferior pulvinar, as well as V1, also showed dense VGLUT2 terminal labeling as well (Marion et al, 2012). Feedback or modulatory projections from V1 primarily arise in layers 5 and 6 and terminate diffusely in the LGN and superior colliculus, as described above, and these projections are dominated by VGLUT1. In V2, feedforward connections largely arise in the superficial layers, which expressed both VGLUT1 and VGLUT2, while feedback projections largely arise in the deep layers, which almost exclusively expressed VGLUT1. Future studies will help to elucidate the distinctions between efferent projections from cortical visual areas and their respective VGLUT isoforms, but both VGLUT1 and VGLUT2 do appear to characterize specific types of glutamatergic projections from V1 and V2.

The pulvinar nucleus of primates consists of several subnuclei with distinct afferent and efferent projections to multiple cortical areas. The majority of its visually related driving and modulatory input arises from projection neurons in the deep layers of cortical areas (Levitt et al, 1995; Lund and Boothe, 1975; Van Horn and Sherman, 2004), which terminate primarily in the lateral and inferior pulvinar. Projections from layer 5 of V1 to the pulvinar are classified as driving projections while projections from layer 6 of V2 to the pulvinar are largely feedback or modulatory in nature. Large VGLUT2-positive neurons in layer 5 of V1 are the likely source of the driving pulvinar input (Lund et al, 1975), while smaller VGLUT1-positive neurons in layer 6 of V2 are the source of modulatory input to these two pulvinar divisions. Efferent projections from the pulvinar to V2 are feedforward or driving connections, while projections from the pulvinar to V1 are modulatory projections instead. Dense VGLUT2 terminal labeling in layer 4 of V2 closely resembles the pattern of pulvinar terminations in this area, while VGLUT1 terminal labeling in layers 1, 3 and 5 of V1 resembles pulvinar projections to V1 instead. Although further studies are necessary to

isolate individual afferent and efferent projections of the visual pulvinar, it appears that driving and modulatory projections from this nucleus are also differentially characterized by VGLUT1 and VGLUT2.

There are several anatomical and functional characteristics of driving and modulating projections, independent of the source of the projection, that also match the physiological properties of VGLUT1 and VGLUT2 within a synapse (Blakely and Edwards, 2012; Fremeau et al, 2004; Hnasko and Edwards, 2012 for review). For example, driving inputs tend to have large excitatory post-synaptic potentials (EPSPs) with a high probability of neurotransmitter release and paired-pulse depression (Sherman and Guillery, 2006, 2011; Viaene et al, 2011a; Viaene et al, 2011b), and VGLUT2 is exclusively expressed at synapses with a high probability of glutamate release (Fremeau et al, 2001). Conversely, modulatory inputs tend to have smaller EPSPs with a lower probability of neurotransmitter release, and VGLUT1 is localized to synapses with the same properties. Driving inputs also exhibit paired-pulse depression (Sherman and Guillery, 2006), as do VGLUT2-positive synapses (Graziano et al, 2008), while modulatory inputs exhibit paired-pulse depression, which is found in VGLUT1-positive synapses (Sherman and Guillery, 2011; Santos et al, 2009). Many of these characteristics now define class 1 and class 2 type projections in sensory systems (Sherman and Guillery, 2011) and VGLUT1 and VGLUT2 may be unique markers for each type. Thus, VGLUT1 and VGLUT2 may differentiate between class 1 and class 2 projections, and could give rise to some of the physiological properties seen in these driving and modulatory connections as well.

5. Conclusion

The discrete distributions of VGLUT1 and VGLUT2 clearly identify individual structures in the macaque visual system, as well as subdivisions within each area or nucleus. Additionally, VGLUT1 and VGLUT2 appear to characterize modulatory and driving connections respectively, in glutamatergic projections between visual cortical areas and subcortical nuclei.

References

Adams MM, Hof PR, Gattass R, et al. Visual cortical projections and chemoarchitecture of macaque monkey pulvinar. J Comp Neurol. 2000; 419:377–393. [PubMed: 10723012]

Aihara Y, Mashima H, Onda H, et al. Molecular cloning of a novel brain-type Na^+-dependent inorganic phosphate cotransporter. J Neurochem. 2000; 74:2622–2625. [PubMed: 10820226]

Anderson JC, Martin KAC. The synaptic connections between cortical areas V1 and V2 in macaque monkey. J Neurosci. 2009; 29:11283–11293. [PubMed: 19741135]

Balaram P, Hackett TA, Kaas JH. VGLUT1 mRNA and protein expression in the visual system of prosimian galagos (*Otolemur garnetti*). Eye Brain. 2011; 3:81–98. [PubMed: 22912561]

Balaram P, Takahata T, Kaas JH. VGLUT2 mRNA and protein expression in the visual thalamus and midbrain of prosimian galagos (*Otolemur garnetti*). Eye Brain. 2011; 3:5–15. [PubMed: 22984342]

Baldwin MK, Wong P, Reed JL, Kaas JH. Superior colliculus connections with visual thalamus in gray squirrels (Sciurus carolinensis): evidence for four subdivisions within the pulvinar complex. J Comp Neurol. 2011; 519:1071–1094. [PubMed: 21344403]

Bellocchio EE, Reimer RJ, Fremeau RT, Edwards RH. Uptake of glutamate into synaptic vesicles by an inorganic phosphate transporter. Science. 2000; 289:957–960. [PubMed: 10938000]

Bender DB. Visual activation of neurons in the primate pulvinar depends on cortex but not colliculus. Brain Res. 1983; 279:258–261. [PubMed: 6640346]

Benevento LA, Fallon JH. The ascending projections of the superior colliculus in the rhesus monkey (Macaca Mulatta). J Comp Neurol. 1975; 160:339–361. [PubMed: 1112928]

Benevento LA, Standage GP. The organization of projections of the retinorecipient and nonretinorecipient nuclei of the pretectal complex and layers of the superior colliculus to the lateral pulvinar and medial pulvinar in the macaque monkey. 217:307–336.

Benevento LA, Yoshida K. The afferent and efferent organization of the lateral geniculo-prestriate pathways in the macaque monkey. Comp Neurol. 1981; 203:455–474.

Berman RA, Wurtz RH. Functional identification of a pulvinar path from superior colliculus to cortical area MT. J Neurosci. 2010; 30:6342–6354. [PubMed: 20445060]

Bernard A, Lubbers LS, Tanis KQ, et al. Transcriptional architecture of the primate neocortex. Neuron. 2012; 73:1083–1099. [PubMed: 22445337]

Bickford ME, Ramcharan E, Godwin DW, et al. Neurotransmitters contained in the subcortical extraretinal inputs to the monkey lateral geniculate nucleus. J Comp Neurol. 2000; 424:701–717. [PubMed: 10931491]

Blakely RD, Edwards RH. Vesicular and plasma membrane transporters for neurotransmitters. Cold Spring Harb Perspect Biol. 2012; 4 a005595.

Blasdel GG, Lund JS. Termination of afferent axons in macaque striate cortex. J Neurosci. 1983; 3:1389–1413. [PubMed: 6864254]

Brodmann, K. Vergleichende Lokalisationlehre der Grosshirnrinde. Barth: Leipzig; 1909.

Bryant KL, Suwyn C, Reding KM, et al. Evidence for Ape and Human specializations in geniculostriate projections from VGLUT2 immunohistochemistry. Brain Behav Evol. 2012; 80:210–221. [PubMed: 22889767]

Bullier J, Kennedy H. Projection of the lateral geniculate nucleus onto cortical area V2 in the macaque monkey. 1983; 53:168–172.

Bullier, J. Communications between cortical areas of the visual system. In: Chalupa, LM.; Werner, JS., editors. The Visual Neurosciences. Cambridge MA: MIT Press; 2004. p. 522-540.

Callaway EM. Local circuits in primary visual cortex of the macaque monkey. Ann Rev Neurosci. 1998; 21:47–74. [PubMed: 9530491]

Campos-Ortega JA, Hayhow WR. On the organization of the visual cortical projection to the pulvinar in Macaca mulatta. Brain Behav Evol. 1972; 6:394–423. [PubMed: 4196833]

Casagrande, VA.; Kaas, JH. The afferent, efferent, and intrinsic connections of primary visual cortex in primates. In: Peters, A.; Rockland, KS., editors. Cerebral Cortex. Plenum Press; 1994.

Casagrande, VA.; Khaytin, I.; Boyd, J. The evolution of parallel visual pathways in the brains of primates. In: Preuss, TM.; Kaas, JH., editors. Evolution of the Nervous System. Elsevier, Inc.; 2006.

Casagrande VA, Yazar F, Jones KD, Ding Y. The morphology of the koniocellular axon pathway in the macaque monkey. Cereb Cortex. 2007; 17:2334–2345. [PubMed: 17215477]

Casagrande VA. A third parallel visual pathway to primate area V1. Trends Neurosci. 1994; 17:305–310. [PubMed: 7524217]

Conley M, Fitzpatrick D. Morphology of retinogeniculate axons in the macaque. Vis Neurosci. 1989; 2:287–296. [PubMed: 2562150]

Cusick CG, Scripter JL, Darensbourg JG, Weber JT. Chemoarchitectonic subdivisions of the visual pulvinar in monkeys and their connectional relations with the middle temporal and rostral dorsolateral visual areas, MT and DLr. J Comp Neurol. 1993; 336:1–30. [PubMed: 8254107]

Danbolt NC, Storm-Mathisen J, Ottersen OP. Sodium/potassium-coupled glutamate transporters, a “new” family of eukaryotic proteins: do they have “new” physiological roles and could they be new targets for pharmacological intervention? Prog Brain Res. 1994; 100:53–60. [PubMed: 7938534]

Davanger S, Manahan-Vaughan D, Mulle C, et al. Protein trafficking, targeting, and interaction at the glutamate synapse. Neurosci. 2009; 158:1–3.

DeYoe EA, Van Essen DC. Segregation of efferent connections and receptive field properties in visual area V2 of the macaque. Nature. 1985; 317:58–61. [PubMed: 2412132]

Felleman DJ, Van Essen DC. Distributed hierarchical processing in the primate cerebral cortex. Cereb Cortex. 1991; 1:1–47. [PubMed: 1822724]

Fitzpatrick D, Usrey WM, Schofield BR, Einstein G. The sublaminar organization of corticogeniculate neurons in layer 6 of macaque striate cortex. Vis Neurosci. 1994; 11:307–315. [PubMed: 7516176]

Fremeau RT, Kam K, Qureshi T, et al. Vesicular glutamate transporters 1 and 2 target to functionally distinct synaptic release sites. Science. 2004; 304:1815–1819. [PubMed: 15118123]

Fremeau RT, Troyer MD, Pahner I, et al. The expression of vesicular glutamate transporters define two classes of excitatory synapse. Neuron. 2001; 31:247–260. [PubMed: 11502256]

Fremeau RT, Voglmaier S, Seal RP, Edwards RH. VGLUTs define subsets of excitatory neurons and suggest novel roles for glutamate. Trends Neurosci. 2004; 27:98–103. [PubMed: 15102489]

Fremeau RT, Burman J, Qureshi T, et al. The identification of vesicular glutamate transporter 3 suggests novel modes of signaling by glutamate. Proc Natl Acad Sci. 2002; 99:14488–14493. [PubMed: 12388773]

Freund TF, Martin KA, Soltesz I, et al. Arborisation pattern and postsynaptic targets of physiologically identified thalamocortical afferents in striate cortex of the macaque monkey. J Comp Neurol. 1989; 289:315–336. [PubMed: 2808770]

Fries W. Cortical projections to the superior colliculus in the macaque monkey: a retrograde study using horseradish peroxidase. J Comp Neurol. 1984; 230:55–76. [PubMed: 6096414]

Fyk-Kolodziej B, Szhagaryan A, Qin P, Pourcho RG. Immunocytochemical localization of three vesicular glutamate transporters in the cat retina. J Comp Neurol. 2004; 475:518–530. [PubMed: 15236233]

Garcia-Marin V, Ahmed TH, Afzal YC, Hawken MJ. Distribution of vesicular glutamate transporter 2 (VGluT2) in the primary visual cortex of the macaque and human. J Comp Neurol. 2013; 521:130–151. [PubMed: 22684983]

Gong J, Jellali A, Mutterer J, et al. Distribution of vesicular glutamate transporters in rat and human retina. Brain Res. 2006; 1082:73–85. [PubMed: 16516863]

Graham J, Lin CS, Kaas JH. Subcortical projections of six visual cortical areas in the owl monkey, *Aotus Trivirgatus*. J Comp Neurol. 1989; 187:557–580. [PubMed: 114555]

Graham J. Some topographical connections of the striate cortex with subcortical structures in *Macaca fascicularis*. Exp Brain Res. 1982; 47:1–14. [PubMed: 7117434]

Gras C, Herzog E, Bellenchi GC, Bernard V, Ravassard P, Pohl M, et al. A third vesicular glutamate transporter expressed by cholinergic and serotonergic neurons. Neurosci. 2002; 22:5442–5451.

Gutierrez C, Yaun A, Cusick CG. Neurochemical subdivisions of the inferior pulvinar in macaque monkeys. J Comp Neurol. 1995; 363:545–562. [PubMed: 8847417]

Hackett TA, de la Mothe LA. Regional and laminar distribution of the vesicular glutamate transporter, VGLuT2, in the macaque monkey auditory cortex. J Comp Neurol. 2009; 38:106–116.

Hackett TA, Takahata T, Balaram P. VGLUT1 and VGLUT2 mRNA expression in the primate auditory pathway. Hear Res. 2011; 274:129–141. [PubMed: 21111036]

Harting JK, Casagrande VA, Weber JT. The projection of the primate superior colliculus upon the dorsal lateral geniculate nucleus: autoradiographic demonstration of interlaminar distribution of tectogeniculate neurons. Brain Res. 1978; 150:593–599. [PubMed: 79427]

Harting JK, Huerta MF, Frankfurter AJ, et al. Ascending pathways from the monkey superior colliculus: an autoradiographic analysis. J Comp Neurol. 1980; 192:853–882. [PubMed: 7419758]

Harting JK, Huerta MF, Hashikawa T, Van Lieshout DP. Projection of the mammalian superior colliculus upon the dorsal lateral geniculate nucleus: organization of tectogeniculate pathways in nineteen species. 1991; 304:275–306.

Hässler, R. Comparative anatomy of the central visual system in day- and night-active primates. In: Hassler; Stephen, editors. Evolution of the Forebrain. Stuttgart: Thieme; 1967. p. 419-434.

Hendrickson AE, Wilson JR, Ogren MP. The neuroanatomical organization of pathways between the dorsal lateral geniculate nucleus and visual cortex in Old World and New World primates. J Comp Neurol. 1978; 182:123–136. [PubMed: 100530]

Herzog E, Bellenchi GC, Gras C, et al. The existence of a second vesicular glutamate transporter specifies subpopulations of glutamatergic neurons. J Neurosci. 2001; 21:RC181. [PubMed: 11698619]

Herzog E, Gilchrist J, Gras C, et al. Localization of VGLUT3, the vesicular glutamate transporter type 3, in the rat brain. Neurosci. 2004; 123:983–1002.

Hevner RF, et al. Beyond laminar fate: toward a molecular classification of cortical projection/pyramidal neurons. Dev Neurosci. 2003; 25:139–151. [PubMed: 12966212]

Hevner RF. Layer-specific markers as probes for neuron-type identity in human neocortex and malformations of cortical development. J Neuropathol Exp Neurol. 2007; 66:101–109. [PubMed: 17278994]

Hnasko TS, Edwards RH. Neurotransmitter corelease: mechanism and physiological role. Ann Rev Physiol. 2012; 74:225–243. [PubMed: 22054239]

Hubel DH, LeVay S, Wiesel TN. Mode of termination of retinotectal fibers in macaque monkey: an autoradiographic study. Brain Res. 1975; 96:25–40. [PubMed: 809107]

Ito T, Bishop DC, Oliver DL. Expression of glutamate and inhibitory amino acid vesicular transporters in the rodent auditory brainstem. J Comp Neurol. 2011; 519:316–340. [PubMed: 21165977]

Kaas JH, Huerta MF, Weber JT, Harting JK. Patterns of retinal terminations and laminar organization of the lateral geniculate nucleus of primates. J Comp Neurol. 1978; 182:517–554. [PubMed: 102662]

Kaas JH, Lyon DC. Pulvinar contributions to the dorsal and ventral streams of visual processing in primates. Brain Res Rev. 2007; 55:285–296. [PubMed: 17433837]

Kaas, JH. The Evolution of Visual Cortex in Primates. In: Kremers, J., editor. The Primate Visual System. CRC Press; 2005.

Kaneko T, Fujiyama F. Complementary distribution of vesicular glutamate transporters in the central nervous system. Neurosci Res. 2001; 42:243–250. [PubMed: 11985876]

Krubitzer LA, Kaas JH. Cortical integration of parallel pathways in the visual system of primates. Brain Res. 1989; 478:161–165. [PubMed: 2466529]

Kubota Y, Kawaguchi Y. Three classes of GABAergic interneurons in neocortex and striatum. Jpn J Physiol. 1994; 44:S145–S148. [PubMed: 7538606]

Lein ES, Hawrylycz MJ, Ao N, et al. Genome-wide atlas of gene expression I the adult mouse brain. Nature. 2007; 445:168–176. [PubMed: 17151600]

Levitt JB, Lund JS, Yoshioka T. Anatomical substrates for early stages in cortical processing of visual information in the macaque monkey. Behav Brain Res. 1996; 76:5–19. [PubMed: 8734040]

Levitt JB, Yoshioka T, Lund JS. Connections between the pulvinar complex and cytochrome oxidase defined compartments in visual area V2 of macaque monkey. Exp Brain Res. 1995; 104:419–430. [PubMed: 7589294]

Lin CS, Kaas JH. Projections from cortical visual areas 17, 18, and MT onto the dorsal lateral geniculate nucleus in owl monkeys. J Comp Neurol. 1977; 173:457–474. [PubMed: 404339]

Lin CS, Kaas JH. The inferior pulvinar complex in owl monkeys: architectonic subdivisions and patterns of input from the superior colliculus and subdivisions of visual cortex. J Comp Neurol. 1979; 187:655–678. [PubMed: 114556]

Livingstone MS, Hubel DH. Specificity of cortico-cortical connections in monkey visual system. Nature. 1983; 304:531–534. [PubMed: 6308468]

Livingstone MS, Hubel DH. Thalamic inputs to cytochrome oxidase-rich regions in monkey visual cortex. Proc Natl Acad Sci. 1982; 79:6098–6101. [PubMed: 6193514]

Lock TM, Baizer JS, Bender DB. Distribution of corticotectal cells in macaque. Exp Brain Res. 2003; 151:455–470. [PubMed: 12851806]

Lund JS, Lund RD, Hendrickson AE, et al. The origin of efferent pathways from the primary visual cortex, Area 17, of the macaque monkey as shown by retrograde transport of horseradish peroxidase. J Comp Neurol. 1975; 164:287–304. [PubMed: 810501]

Lund JS. Local circuit neurons of macaque monkey striate cortex I. Neurons of laminae 4C and 5A. J Comp Neurol. 1987; 257:60–92. [PubMed: 3571519]

Lund JS. Anatomical organization of macaque monkey striate visual cortex. Ann Rev Neurosci. 1988; 11:253–288. [PubMed: 3284442]

Lund JS. Specificity and non-specificity of synaptic connections with mammalian visual cortex. J Neurocytol. 2002; 31:203–209. [PubMed: 12815240]

Lund RD. Synaptic patterns in the superficial layers of the superior colliculus of the monkey, Macaca mulatta. Exp Brain Res. 1972; 15:194–211. [PubMed: 4627199]

Lyon DC, Nassi JJ, Callaway EM. A disynaptic relay from superior colliculus to dorsal stream visual cortex in macaque monkey. Neuron. 2010; 65:270–279. [PubMed: 20152132]

Marion R, Li K, Purushothaman G, et al. Morphological and neurochemical comparisons between pulvinar and V1 projections. J Comp Neurol. 2012; 521:813–832. [PubMed: 22826174]

Marrocco RT, McClurkin JW, Young RA. Spatial properties of superior colliculus cells projecting to the inferior pulvinar and parabigeminal nucleus of the monkey. 1981; 222:150–154.

Masterson SP, Li J, Bickford ME. Synaptic organization of the tectorecipient zone of the rat lateral posterior nucleus. J Comp Neurol. 2009; 515:647–663. [PubMed: 19496169]

Maunsell JHR, Van Essen DC. The connections of the middle temporal visual area (MT) and their relationship to a cortical hierarchy in the macaque monkey. J Neurosci. 1983; 3:2563–2586. [PubMed: 6655500]

May PJ. The mammalian superior colliculus: laminar structure and connections. Prog Brain Res. 2006; 151:31–378.

Miguel-Hidalgo JJ, Senba E, Matsutani S, et al. Laminar and segregated distribution of immunoreactivities for some neuropeptides and adenoine deaminase in the superior colliculus of the rat. J Comp Neurol. 1989; 280:410–423. [PubMed: 2465326]

Ogren MP, Hendrickson AE. The distribution of pulvinar terminals in visual areas 17 and 18 of the monkey. Brain Res. 1977; 137:343–350. [PubMed: 412565]

Olszewski, J. The Thalamus of Macaca Mulatta. Basel, Switzerland: S Karger; 1952.

Partlow GD, Colonnier M, Szabo J. Thalamic projections of the superior colliculus in the rhesus monkey, Macaca mulatta. A light and electron microscopic study. J Comp Neurol. 1977; 72:285–318. [PubMed: 401837]

Pollack JG, Hickey TL. The distribution of retino-collicular axon terminals in the rhesus monkey. 1979; 185:587–602.

Poppel E, Held R, Frost D. Residual visual function after brain wounds involving the central visual pathway in man. Nature. 1985; 243:295–296. [PubMed: 4774871]

Reimer RJ, Fremeau RT Jr, Bellocchio EE, Edwards RH. The essence of excitation. Curr Opin Cell Biol. 2001; 13:417–421. [PubMed: 11454446]

Rockland KS, Pandya DN. Laminar origins and terminations of cortical connections of the occipical lobe in the rhesus monkey. Brain Res. 1979; 179:3–20. [PubMed: 116716]

Rockland, KS. The organization of feedback connections from area V2 (18) to V1 (17). In: Peters, A.; Jones, EG., editors. Cerebral Cortex. New York, NY: Plenum Press; 1994.

Salin PA, Bullier J. Corticocortical connections in the visual system: structure and function. Phys Rev. 1995; 75:107–142.

Santos MS, Li H, Voglmaier SM. Synaptic vesicle protein trafficking at the glutamate synapse. Neuroscience. 2009; 158:189–203. [PubMed: 18472224]

Schäfer MK, Varoqui H, Defamie N, et al. Molecular cloning and functional identification of mouse vesicular glutamate transporter 3 and its expression in subsets of novel excitatory neurons. J Biol Chem. 2002; 277:50734–50748. [PubMed: 12384506]

Seal RP, Edwards RH. The diverse roles of vesicular glutamate transporter 3. Handb Exp Pharmacol. 2006; 175:137–150. [PubMed: 16722234]

Sherman SM, Guillery RW. The role of the thalamus in the flow of information to the cortex. Phil Trans R Soc Lond B Biol Sci. 2002; 357:1695–1708. [PubMed: 12626004]

Sherman, SM.; Guillery, RW. Exploring the thalamus and its role in cortical function. Cambridge, MA: MIT Press; 2006.

Sherman SM, Guillery RW. Distinct functions for direct and transthalamic corticocortical connections. J Neurophysiol. 2011; 106:1068–1077. [PubMed: 21676936]

Sherman SM. The thalamus is more than just a relay. Curr Opin Neurobiol. 2007; 17:417–422. [PubMed: 17707635]

Shipp S, Zeki S. The organization of connections between areas V5 and V1 in macaque monkey visual cortex. Eur J Neurosci. 1989; 1:309–331. [PubMed: 12106142]

Shipp S. Corticopulvinar connections of areas V5, V4, and V3 in the macaque monkeys: a dual model of retinal and cortical topographies. J Comp Neurol. 2001; 439:469–490. [PubMed: 11596067]

Sincich LC, Horton JC. Divided by cytochrome oxidase: A map of the projections from V1 to V2 in macaques. Science. 2002; 295:1734–1737. [PubMed: 11872845]

Sincich LC, Jocson CM, Horton JC. V1 interpatch projections to V2 thick stripes and pale stripes. J Neurosci. 2010; 30:6963–6974. [PubMed: 20484638]

Sincich LC, Park KF, Wohlgemuth MJ, et al. Bypassing V1: a direct geniculate input to area MT. 2004; 7:1123–1128.

Sincich LC, Park KF, Wohlgemuth MJ, Horton JC. Bypassing V1: a direct geniculate input to area MT. Nat Neurosci. 2004; 7:1123–1128. [PubMed: 15378066]

Soares JG, Gattass R, Souza AP, et al. Connectional and neurochemical subdivisions of the pulvinar in Cebus monkeys. Vis Neurosci. 2001; 18:25–41. [PubMed: 11347814]

Stepniewska I, Kaas JH. Architectonic subdivisions of the inferior pulvinar in New World and Old World monkeys. Vis Neurosci. 1997; 14:1043–1060. [PubMed: 9447687]

Stepniewska I, Qi HX, Kaas JH. Do superior colliculus projection zones in the inferior pulvinar project to MT in primates? Eur J Neurosci. 1999; 11:469–480. [PubMed: 10051748]

Stepniewska I, Qi HX, Kaas JH. Projections of the superior colliculus to subdivisions of the inferior pulvinar in New World and Old World monkeys. Vis Neurosci. 2000; 17:529–549. [PubMed: 11016573]

Stepniewska, I. The pulvinar complex. In: Kaas, JH.; Collins, CE., editors. The Primate Visual System. Boca Raton, FL: CRC Press; 2004.

Stoerig P, Cowey A. Blindsight. Curr Biol. 2007; 17:R822–R824. [PubMed: 17925204]

Tamietto M, Cauda F, Corazzini LL, et al. Collicular vision guides nonconscious behavior. J Cogn Neurosci. 2010; 22:888–902. [PubMed: 19320547]

Tochitani S, Liang F, Watakabe A, et al. The occ1 gene is preferentially expressed in the primary visual cortex in an activity-dependent manner: a pattern of gene expression related to the cytoarchitectonic area in the adult macaque neocortex. Eur J Neurosci. 2001; 13:297–307. [PubMed: 11168534]

Trojanowski JO, Jacobson S. Peroxidase labeled subcortical afferents to pulvinar in rhesus monkey. Brain Res. 1975; 97:144–150. [PubMed: 809115]

Valverde, F. The organizing principles of the primary visual cortex in the monkey. In: Peters, A.; Jones, ED., editors. Cerebral Cortex Vol. 3. Visual Cortex. New York: Plenum Press; 1985. p. 207-252.

Van Essen DC. Corticocortical and thalamocortical information flow in the primate visual system. Prog Brain Res. 2005; 149:173–185. [PubMed: 16226584]

Van Essen, DC. Functional organization of primate visual cortex. In: Peters, A.; Jones, ED., editors. Cerebral Cortex Vol. 3, Visual Cortex. New York: Plenum Press; 1985. p. 259-320.

Varoqui H, Schafer MK, Zhu H, et al. Identification of the differentiation-associated Na+/Pi trasporter as a novel vesicular glutamate transporter expressed in a distinct set of glutamatergic synapses. J Neurosci. 2002; 22:142–155. [PubMed: 11756497]

Viaene AN, Petrof I, Sherman SM. Synaptic properties of thalamic input to the subgranular layers of primary somatosensory and auditory cortices in the mouse. J Neurosci. 2011; 31:12738–12747. [PubMed: 21900553]

Viaene AN, Petrof I, Sherman SM. Synaptic properties of thalamic input to layers 2/3 and 4 of primary somatosensory and auditory cortices. J Neurophysiol. 2011; 105:279–292. [PubMed: 21047937]

Warden MK, Young WS III. Distribution of cels containing mRNAs encoding substance P and neurokinin B in the rat central nervous system. J Comp Neurol. 1988; 272:90–113. [PubMed: 2454979]

Wilson ME, Toyne MJ. Retinotectal and corticotectal projections in *Macaca Mulatta*. Brain Res. 1970; 24:395–406. [PubMed: 4099749]

Winfield DA, Rivera-Dominguez M, Powell TP. The termination of geniculocortical fibres in area 17 of the visual cortex in the macaque monkey. 1982; 231:19–32.

Wong-Riley M. Changes in the visual system of monocularly sutured or enucleated cats demonstrable with cytochrome oxidase histochemistry. Brain Res. 1979; 171:11–28. [PubMed: 223730]

Yamamori T. Selective gene expression in regions of primate neocortex: implications for cortical specialization. Prog Neurobiol. 2011; 96:164.

Yukie M, Iwai E. Direct projection from the dorsal lateral geniculate nucleus to the prestriate cortex in macaque monkeys. J Comp Neurol. 1981; 201:81–97. [PubMed: 7276252]

Highlights

- VGLUT1 and VGLUT2 show distinct mRNA and protein expression patterns in the macaque visual system
- VGLUT1 and VGLUT2 distributions identify distinct architectonic divisions within all visual subcortical nuclei and cortical areas
- VGLUT2 predominates in driving or feedforward visual projections, while VGLUT1 predominates in modulatory or feedback projections between visual areas and nuclei

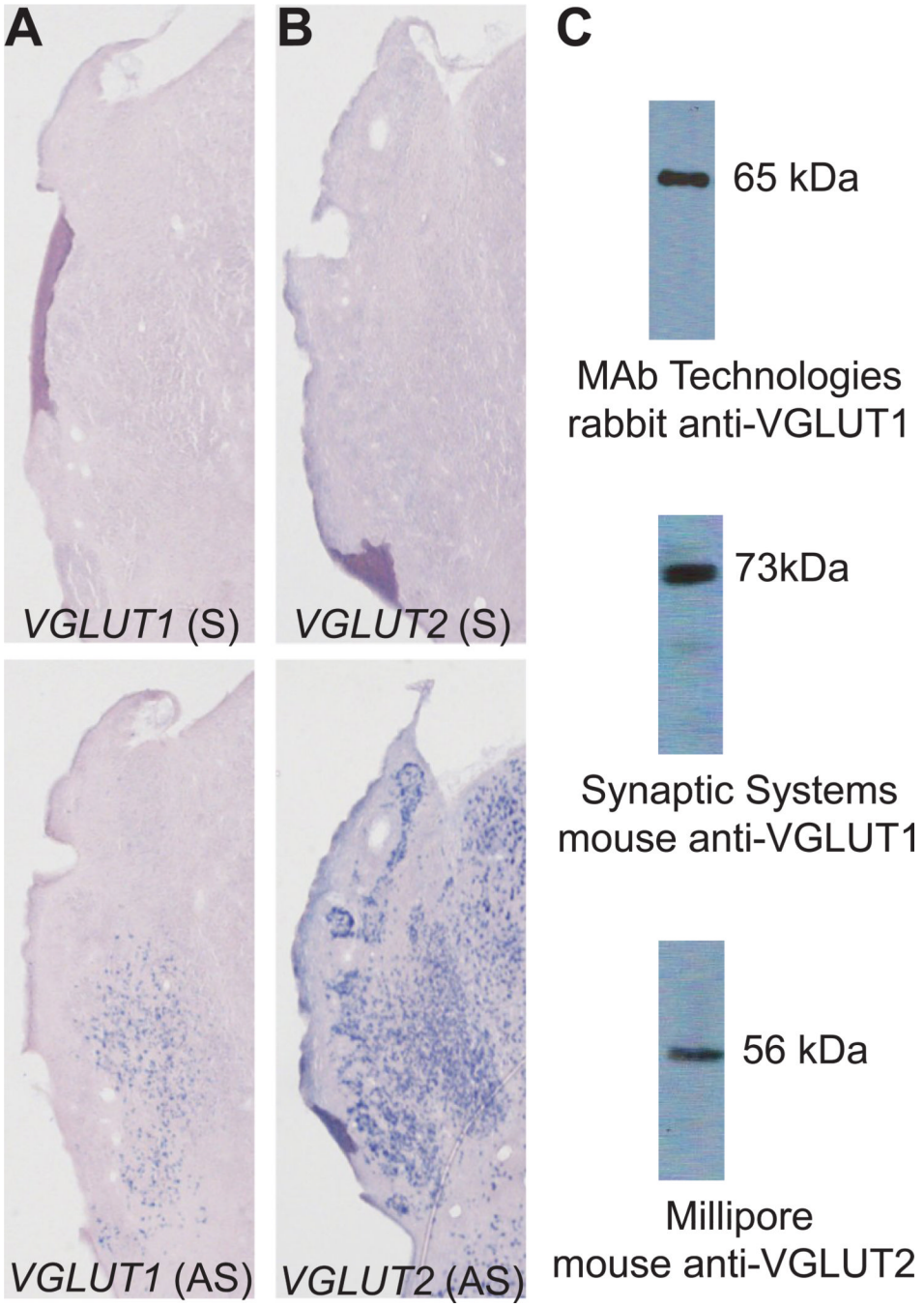

Figure 1.
(A–B) Sense and antisense staining of *VGLUT1* and *VGLUT2* mRNA in macaque thalamus sections confirms probe specificity. (C) Western blotting for VGLUT1 and VGLUT2 protein in macaque cerebellum lysate confirms antibody specificity for both proteins. Abbreviations: S, sense probe; AS, antisense probe.

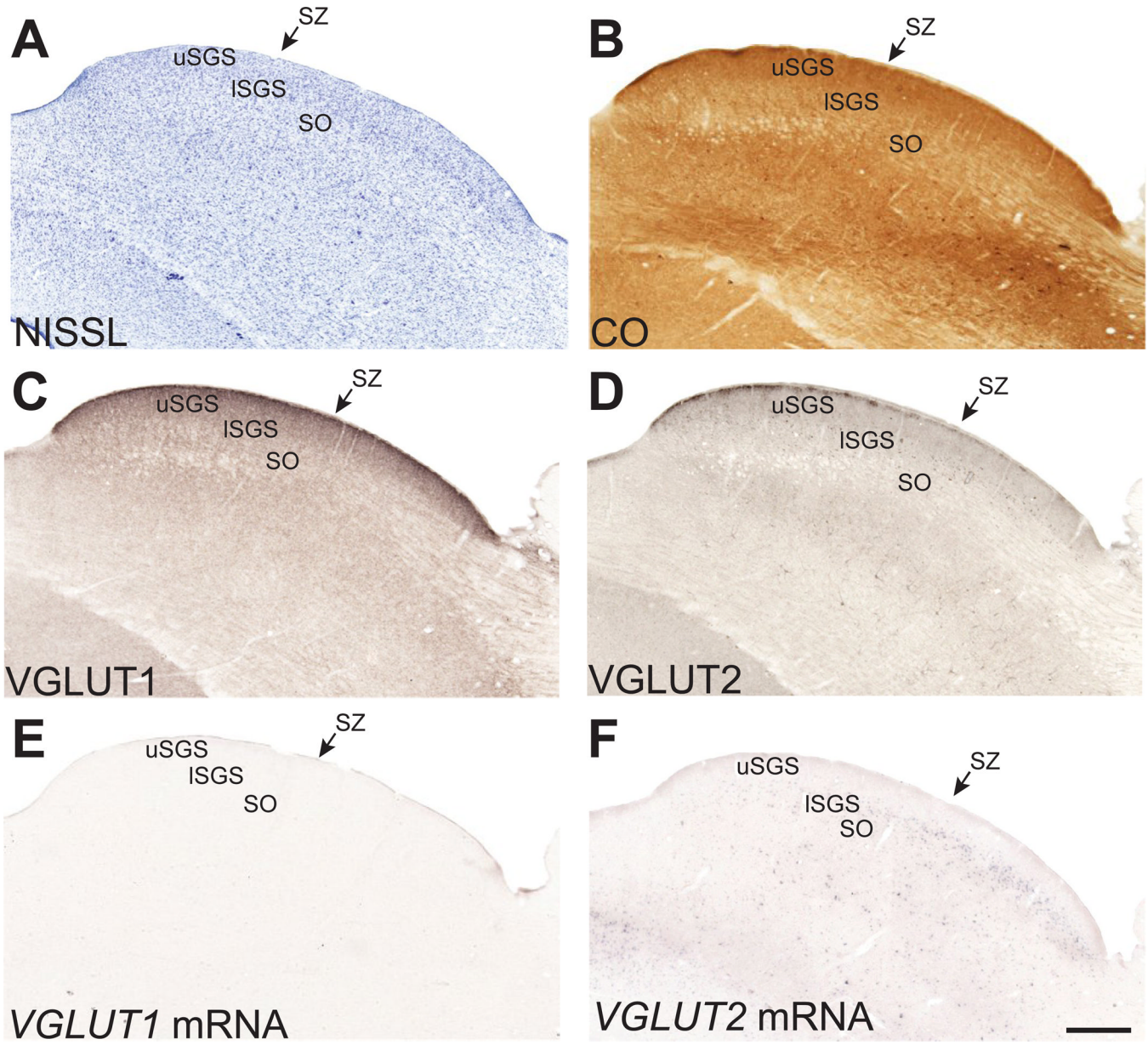

Figure 2.
Low magnification images through the macaque superior colliculus. Scale bar is 1mm, thalamic midline is to the left. Abbreviations: CO, cytochrome oxidase; SZ, zonal layer; uSGS, upper superficial gray layer; 1SGS, lower superficial gray layer; SO, optic layer.

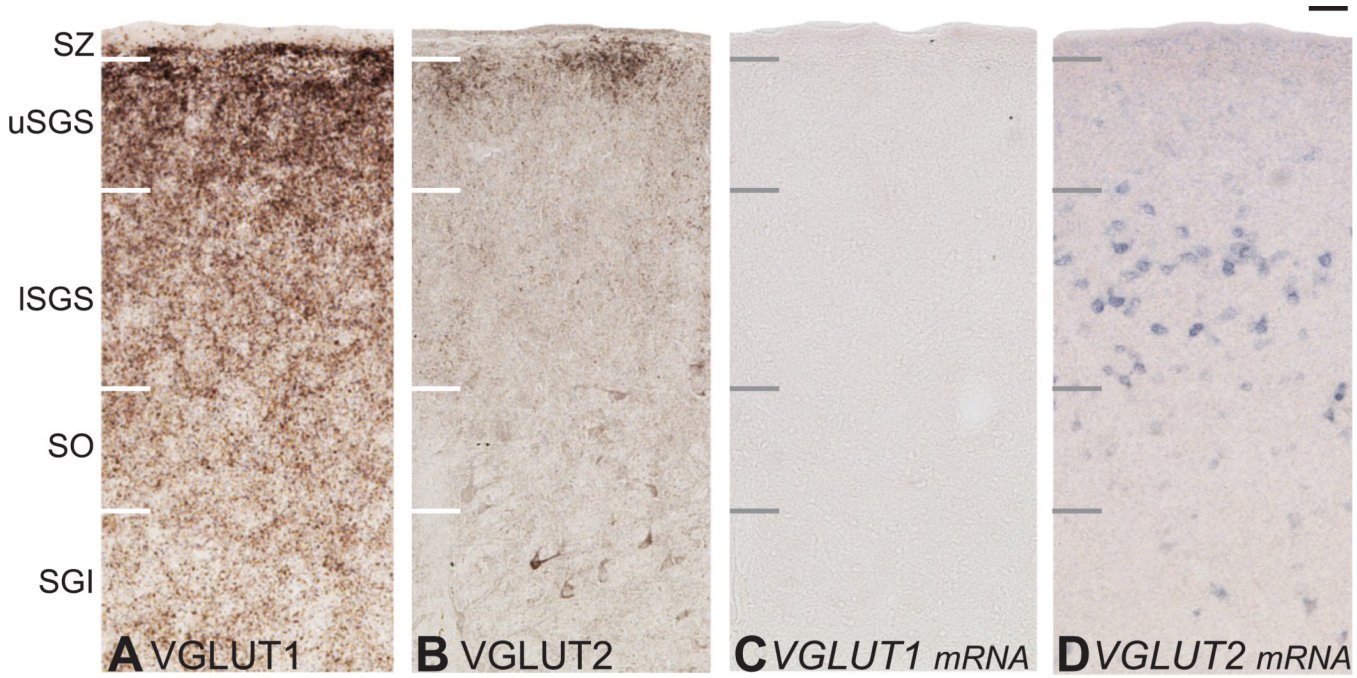

Figure 3.

High magnification images of VGLUT distributions in the superior colliculus. Laminar divisions are listed on the left, scale bar is 25um. Abbreviations: CO, cytochrome oxidase; SZ, zonal layer; uSGS, upper superficial gray layer; lSGS, lower superficial gray layer; SO, optic layer; SGI, intermediate gray layer.

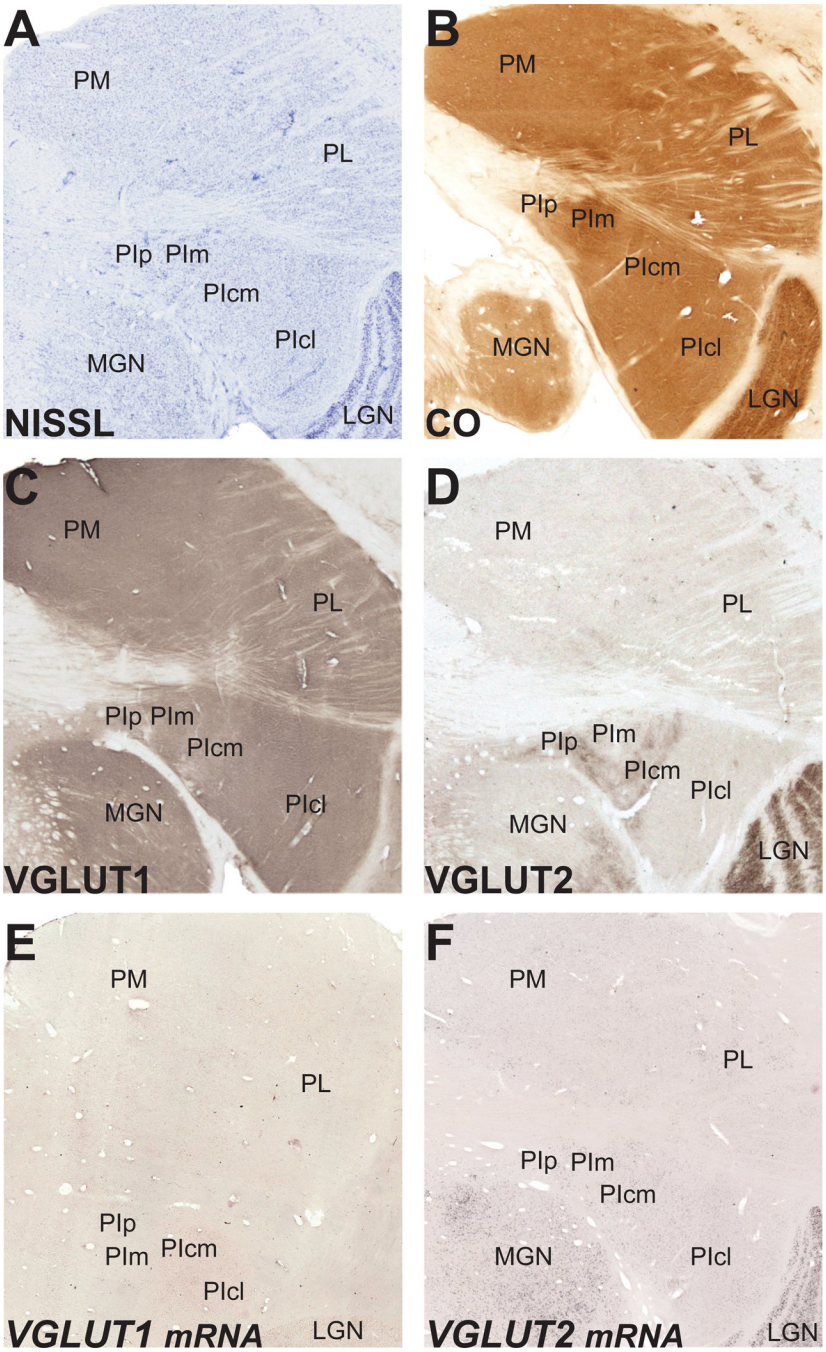

Figure 4.

Low magnification images through the pulvinar complex. Scale bar is 1mm, thalamic midline is to the left. Abbreviations: CO, cytochrome oxidase; PM, medial pulvinar; PL, lateral pulvinar; PIp, posterior inferior pulvinar; PIm, medial inferior pulvinar; PIcm, central medial inferior pulvinar; PIcl, central lateral inferior pulvinar; MGN, medial geniculate nucleus; LGN, lateral geniculate nucleus.

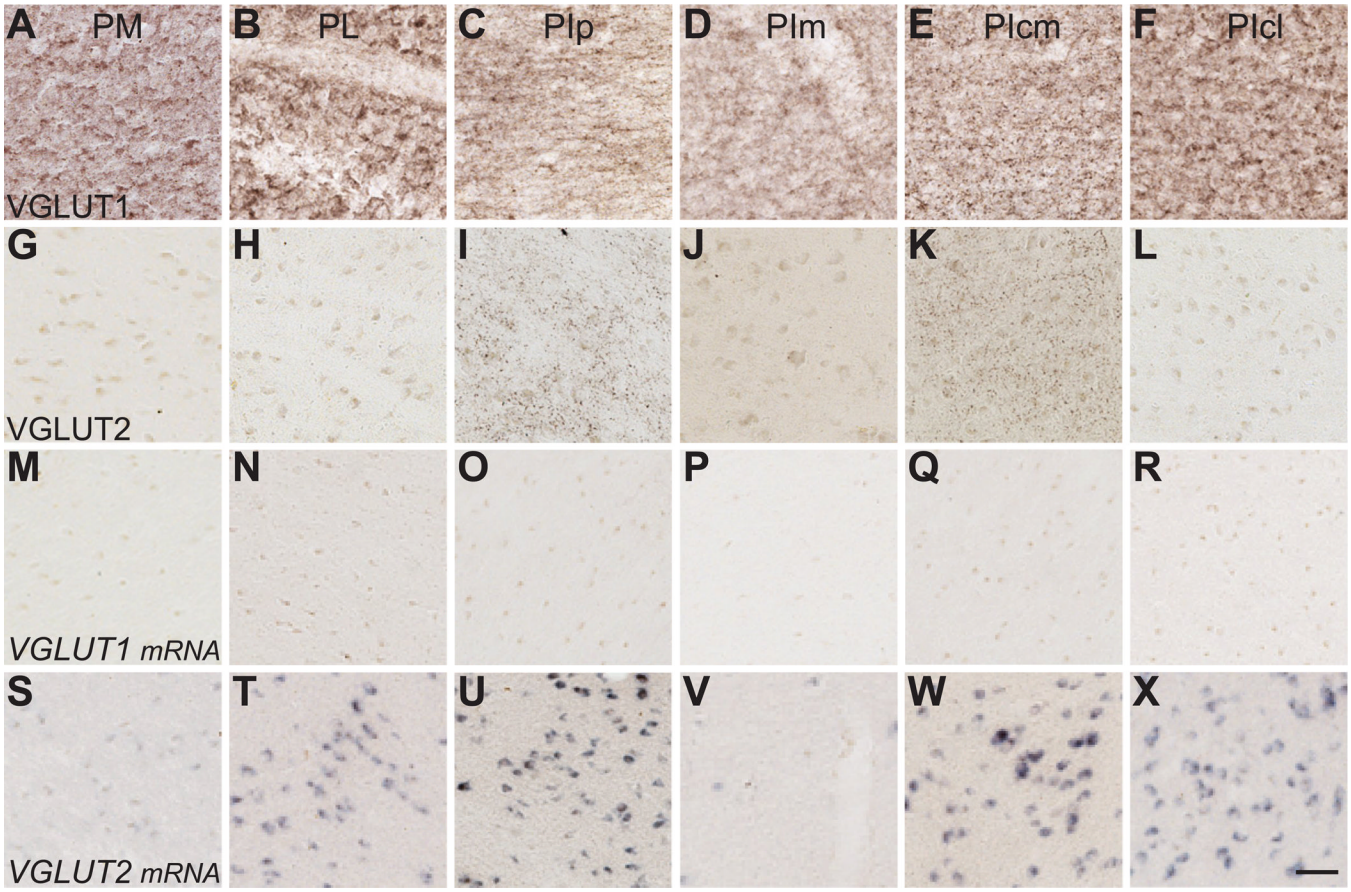

Figure 5.

High magnification images of VGLUT distributions in the pulvinar complex. VGLUT2 protein (A, B) and *VGLUT2* mRNA (A', B') expression distinguish three clear subdivisions in the inferior pulvinar. (C–Z) VGLUT1 and VGLUT2 distributions vary distinctly between medial, lateral, and inferior pulvinar subdivisions. Scale bars are 500um. Abbreviations: CO, cytochrome oxidase; PM, medial pulvinar; PL, lateral pulvinar; PIp, posterior inferior pulvinar; PIm, medial inferior pulvinar; PIcm, central medial inferior pulvinar; PIcl, central lateral inferior pulvinar; dLGN, dorsal lateral geniculate nucleus; MGN, medial geniculate nucleus.

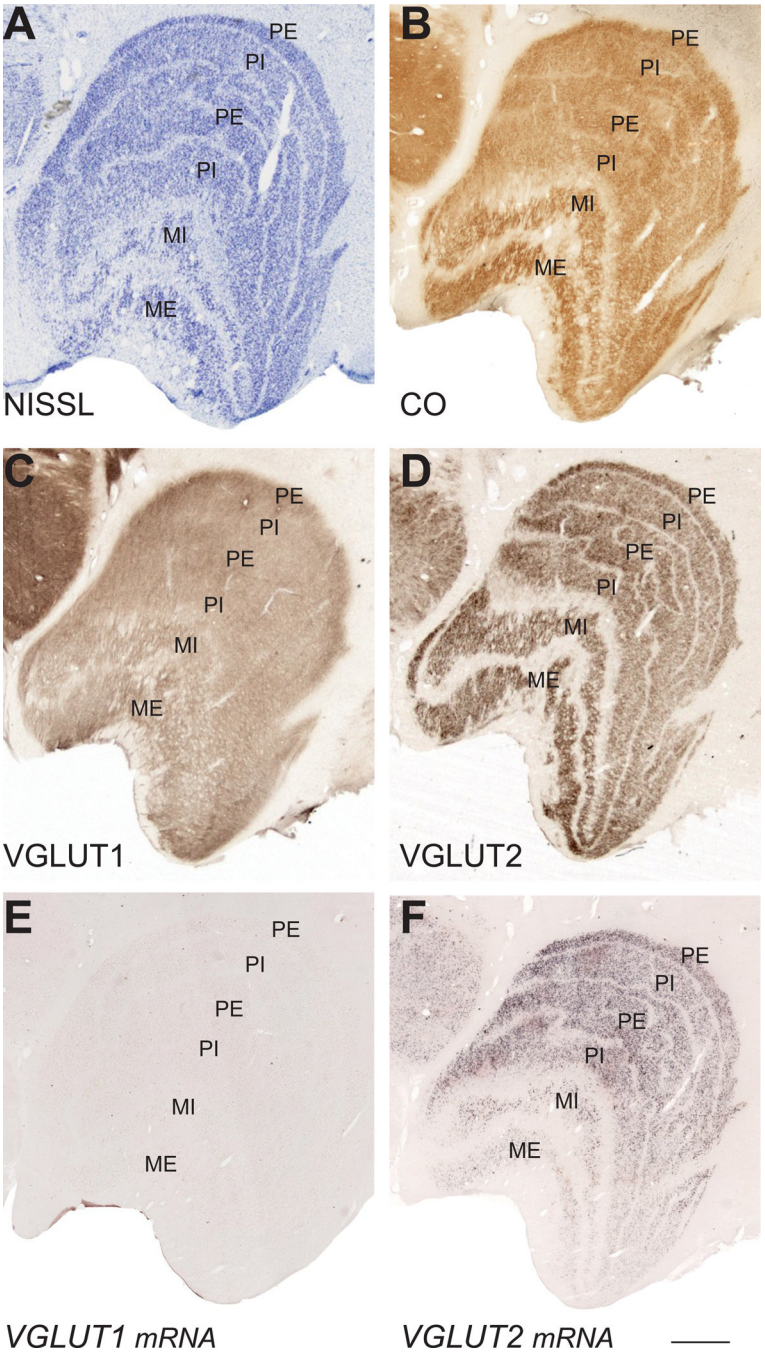

Figure 6.

Low magnification images through the lateral geniculate nucleus (LGN). Scale bar is 1mm, thalamic midline is to the left. Abbreviations: CO, cytochrome oxidase; ME, external magnocellular layer; MI, internal magnocellular layer; PI, internal parvocellular layer; PE, external parvocellular layer.

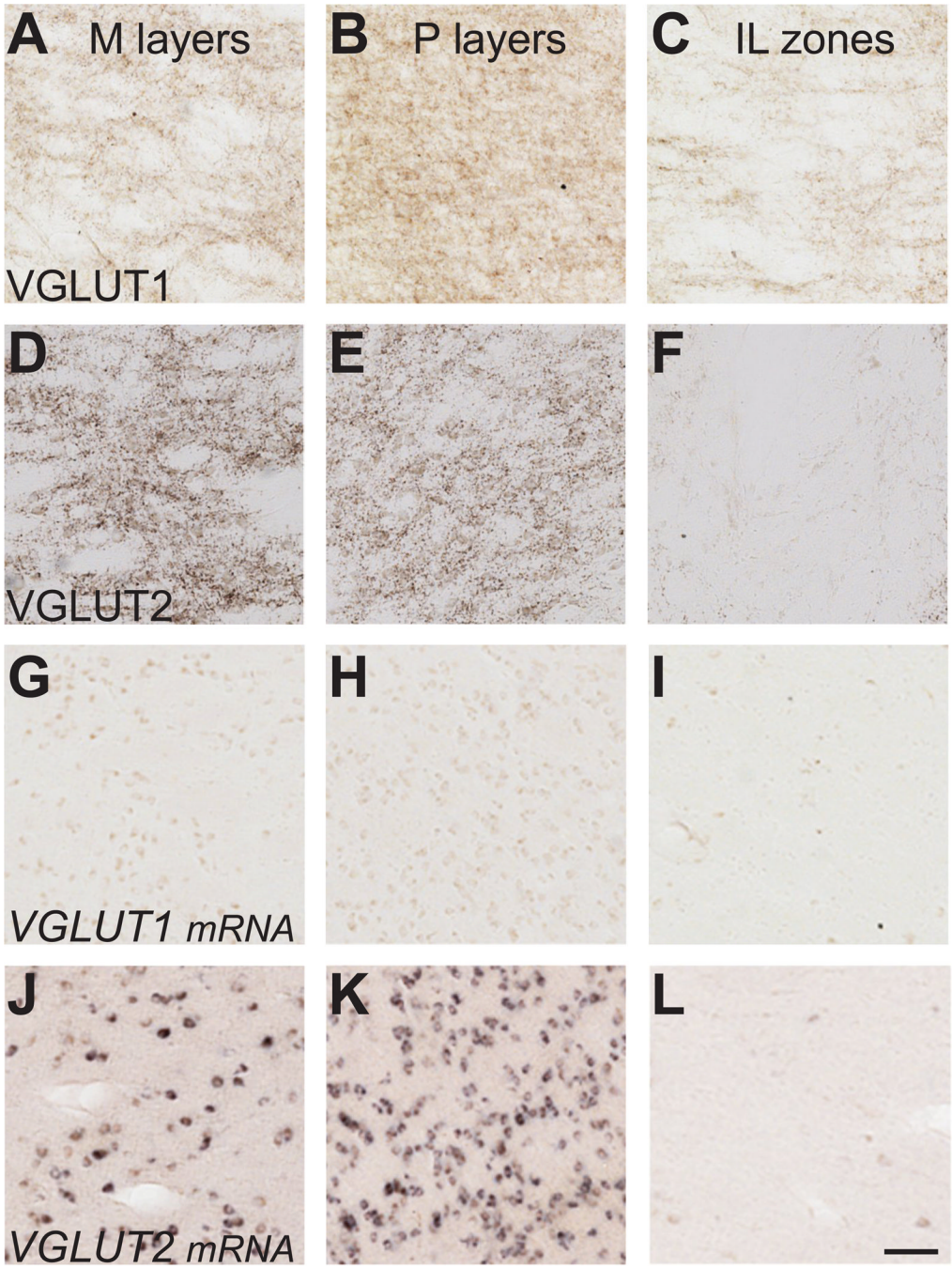

Figure 7.
High magnification images of VGLUT distributions in the LGN. (G–H) Arrowheads show two different cell populations based on cell size. Scale bar is 500um. Abbreviations: CO, cytochrome oxidase; M, magnocellular; P, parvocellular; K, koniocellular.

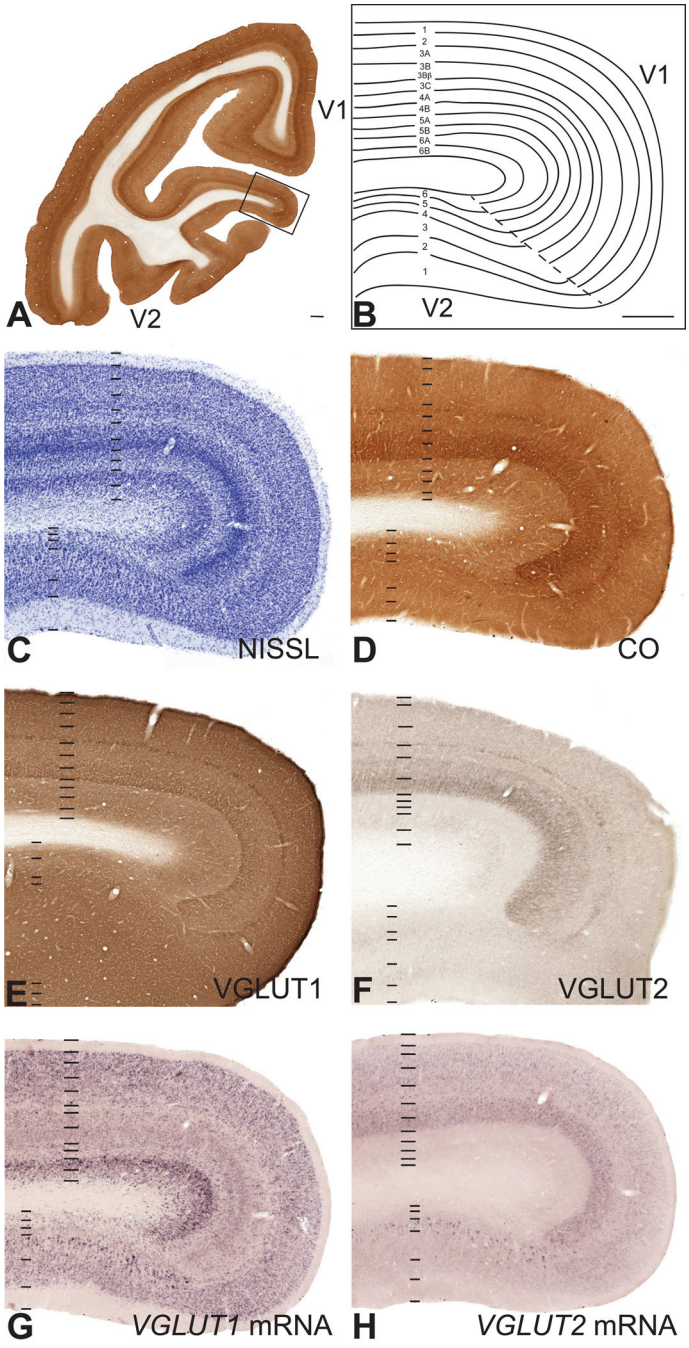

Figure 8.

Low magnification images of V1 and V2. (A) Coronal section of cytochrome oxidase (CO) reactivity in V1 and V2, showing region of interest for panels B–H. (B) Areal and laminar divisions of V1 and V2 in reference to panels C–H, adapted from Casagrande and Kaas (1994). Scale bars in panels A and B are 1mm.

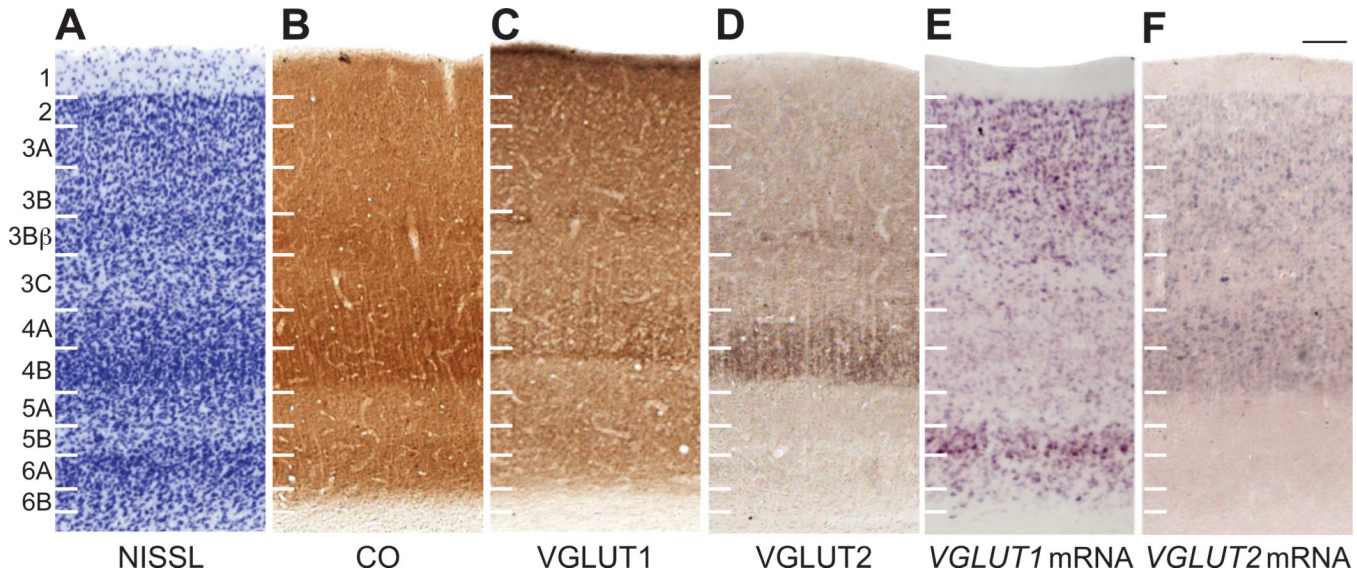

Figure 9.
High magnification images through V1. Laminar divisions indicated on the left, adapted from Casagrande and Kaas (1994). Scale bar is 500um.

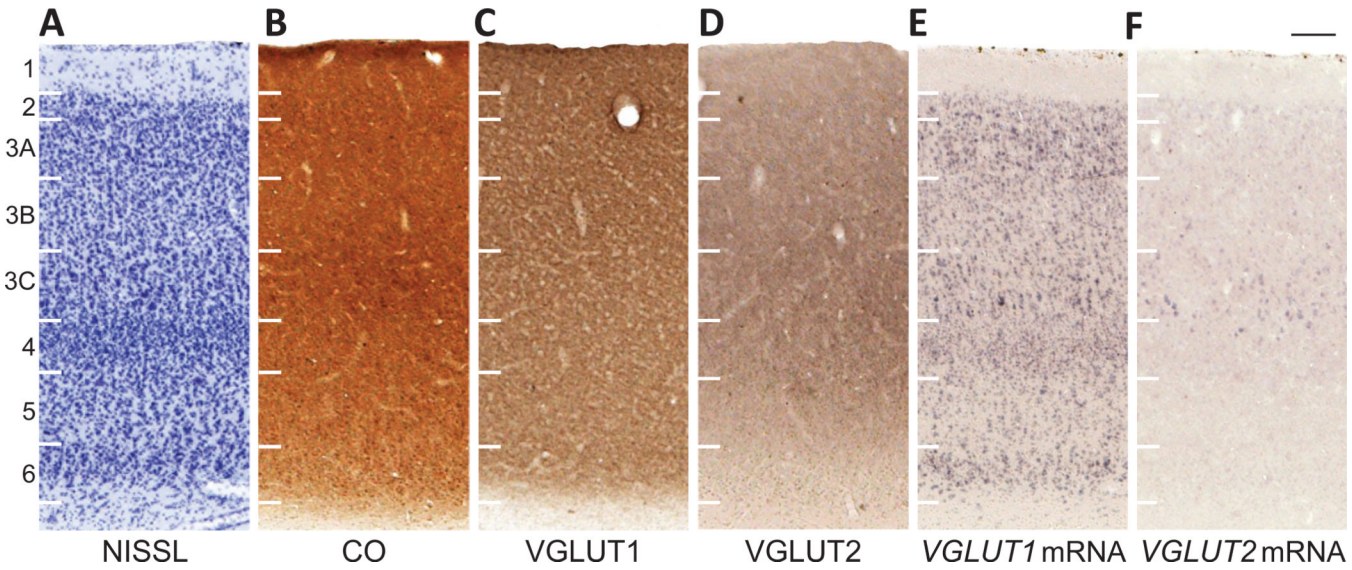

Figure 10.
High magnification images through V2. Laminar divisions indicated on the left, adapted from Casagrande and Kaas (1994). Scale bar is 500um.

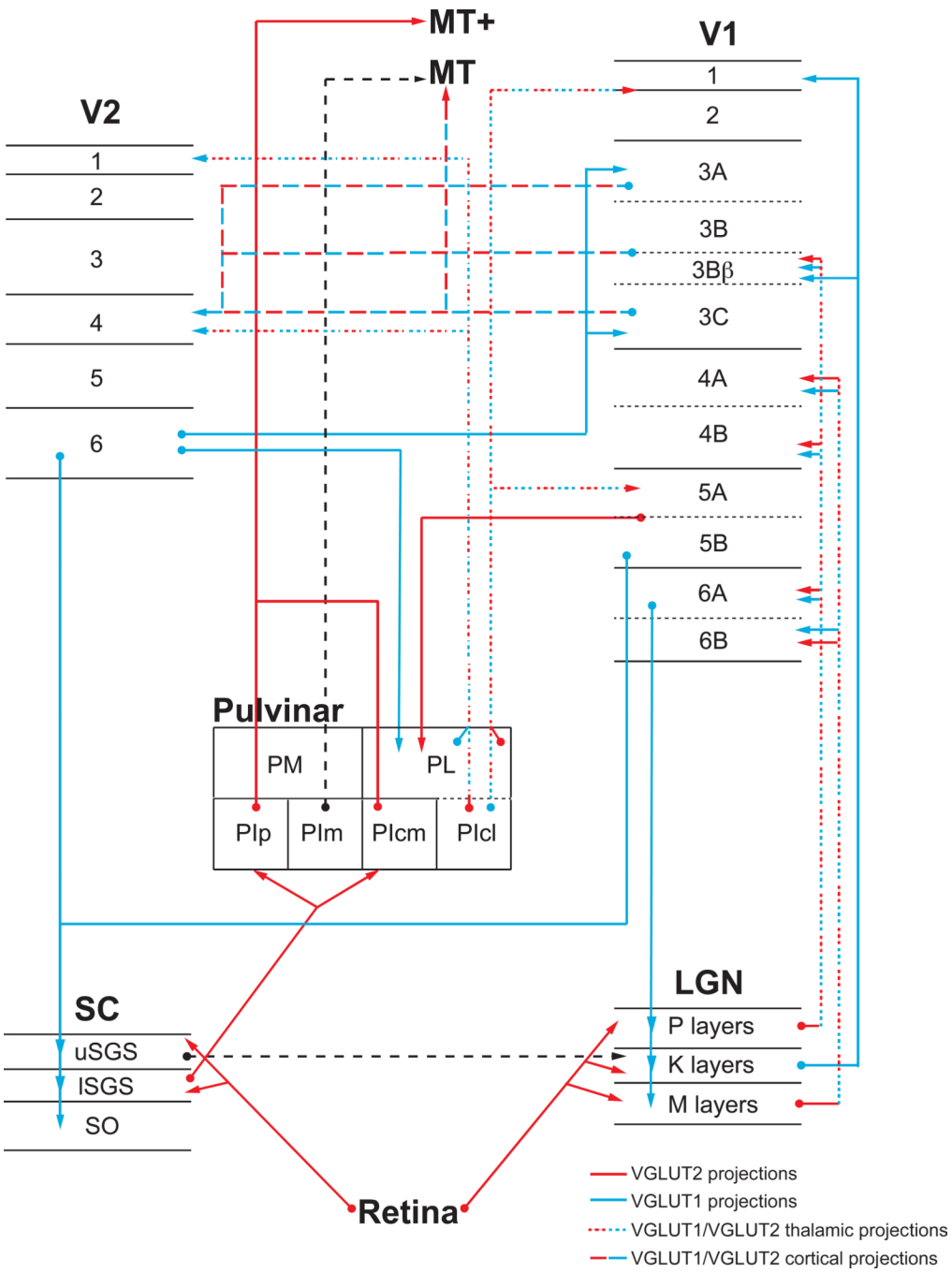

Figure 11.

Summary of major feedforward and feedback projections in the macaque visual system. Circles indicate origin of projection, arrowheads indicate termination of projection. Abbreviations: SC, superior colliculus {uSGS, upper superficial gray layer; lSGS, lower superficial gray layer; SO, optic layer}; LGN, lateral geniculate nucleus {P, parvocellular; K, koniocellular; M, magnocellular}; Pulvinar {PM, medial pulvinar; PL, lateral pulvinar; PIp, posterior inferior pulvinar; PIm, medial inferior pulvinar; PIcm, central medial inferior pulvinar; PIcl, central lateral inferior pulvinar}; V1, area V1; V2, area V2; MT, middle temporal area; MT+, MT associated areas (MTc, MST, FST, etc). Adapted from Casagrande and Kaas, 1994.

Table 1

Commercial antibodies and relative concentrations used for immunohistochemistry and western blotting of VGLUT1 and VGLUT2.

	Primary antibody (IHC, WB)	**Secondary Antibody (IHC)**	**Normal Serum (IHC)**	**Secondary Antibody (WB)**
VGLUT1 (cortex)	Rabbit anti-VGLUT1 (MAb Technologies) 1:3000 IHC 1:1000 WB	Biotinylated goat anti-rabbit IgG (Vector Labs) 1:500	Goat serum (Vector Labs)	HRP-conjugated goat anti-rabbit IgG (Jackson Labs) 1:30,000
VGLUT1 (thalamus, midbrain)	Mouse anti-VGLUT1 (Synaptic Systems) 1:3000 IHC 1:1000 WB	Biotinylated goat anti-mouse IgG (Vector Labs) 1:500	Goat serum (Vector Labs)	HRP-conjugated goat anti-mouse IgG (Jackson Labs) 1:20,000
VGLUT2 (thalamus/midbrain/cortex)	Mouse anti-VGLUT2 (Millipore) 1:5000 IHC 1:2000 WB	Biotinylated horse anti-mouse IgG (Vector Labs) 1:500	Horse serum (Vector Labs)	HRP-conjugated goat anti-mouse IgG (Jackson Labs) 1:30,000